

45V_{IN}, 4A Synchronous Buck Regulator

Features

- 4.6V to 45V Operating Input Voltage Supply
- Up to 4A Output Current
- Integrated High-Side and Low-Side N-Channel MOSFETs
- HyperLight Load[®] (MIC28513-1) and Hyper Speed Control[®] (MIC28513-2) Architecture
- Enable Input and Power Good (PGOOD) Output
- Programmable Current-Limit and Foldback “Hiccup” Mode Short-Circuit Protection
- Built-In 5V Regulator for Single-Supply Operation
- Adjustable 200 kHz to 680 kHz Switching Frequency
- Fixed 5 ms Soft-Start
- Internal Compensation and Thermal Shutdown
- Thermally-Enhanced 24-Pin 3 mm x 4 mm FQFN Package
- -40°C to +125°C Junction Temperature Range

Applications

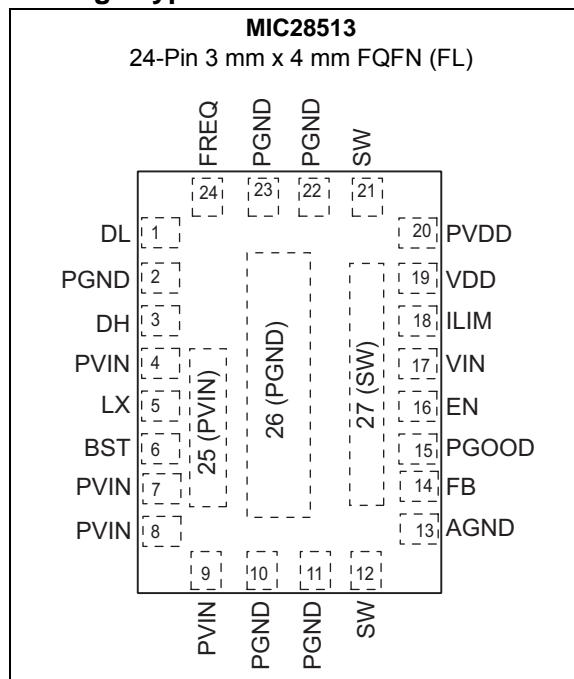
- Industrial Power Supplies
- Distributed Supply Regulation
- Base Station Power Supplies
- Wall Transformer Regulation
- High-Voltage Single-Board Systems

General Description

The MIC28513 is a synchronous step-down switching regulator with internal power switches capable of providing up to 4A output current from a wide input supply range from 4.6V to 45V. The output voltage is adjustable down to 0.8V with a guaranteed accuracy of ±1%. A constant switching frequency can be programmed from 200 kHz to 680 kHz. The MIC28513’s Hyper Speed Control[®] and HyperLight Load[®] architectures allow for high V_{IN} (low V_{OUT}) operation and ultra-fast transient response while reducing the required output capacitance. The MIC28513-1’s HyperLight Load architecture also provides very good light load efficiency.

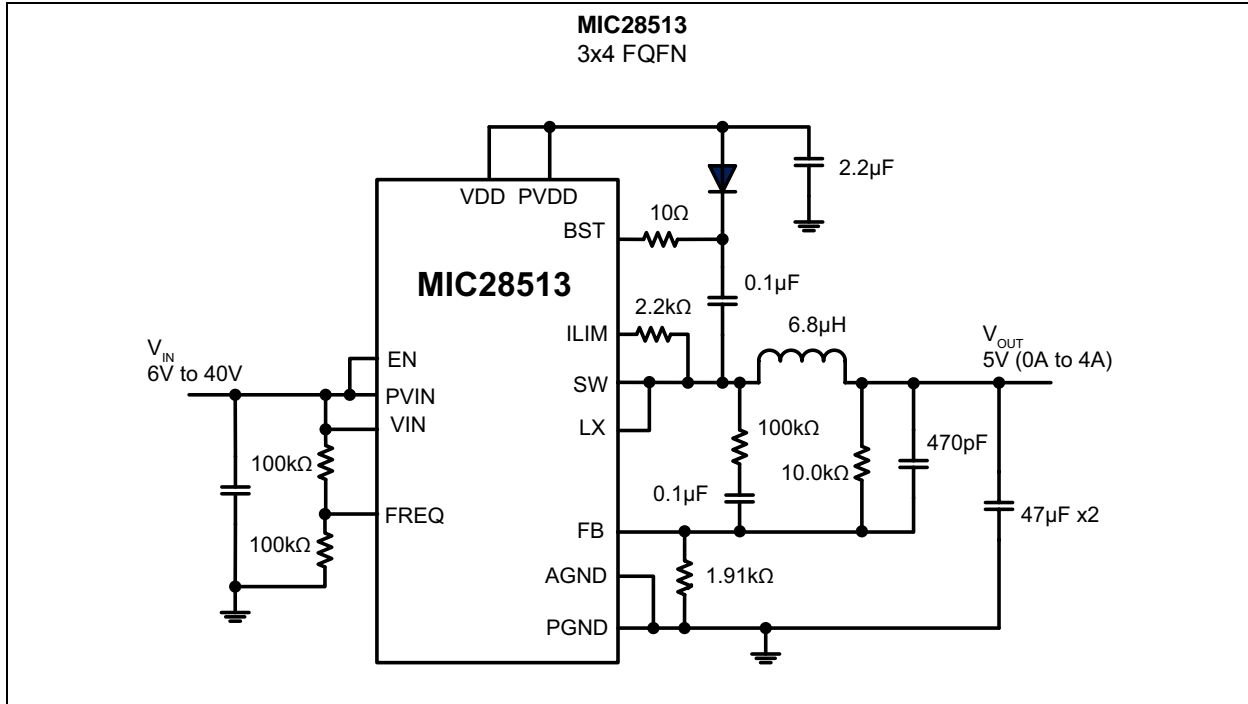
The MIC28513 offers a full suite of features to ensure protection under fault conditions. These include undervoltage lockout to ensure proper operation under power sag conditions, internal soft-start to reduce inrush current, foldback current limit, “hiccup” mode short-circuit protection, and thermal shutdown.

Package Type

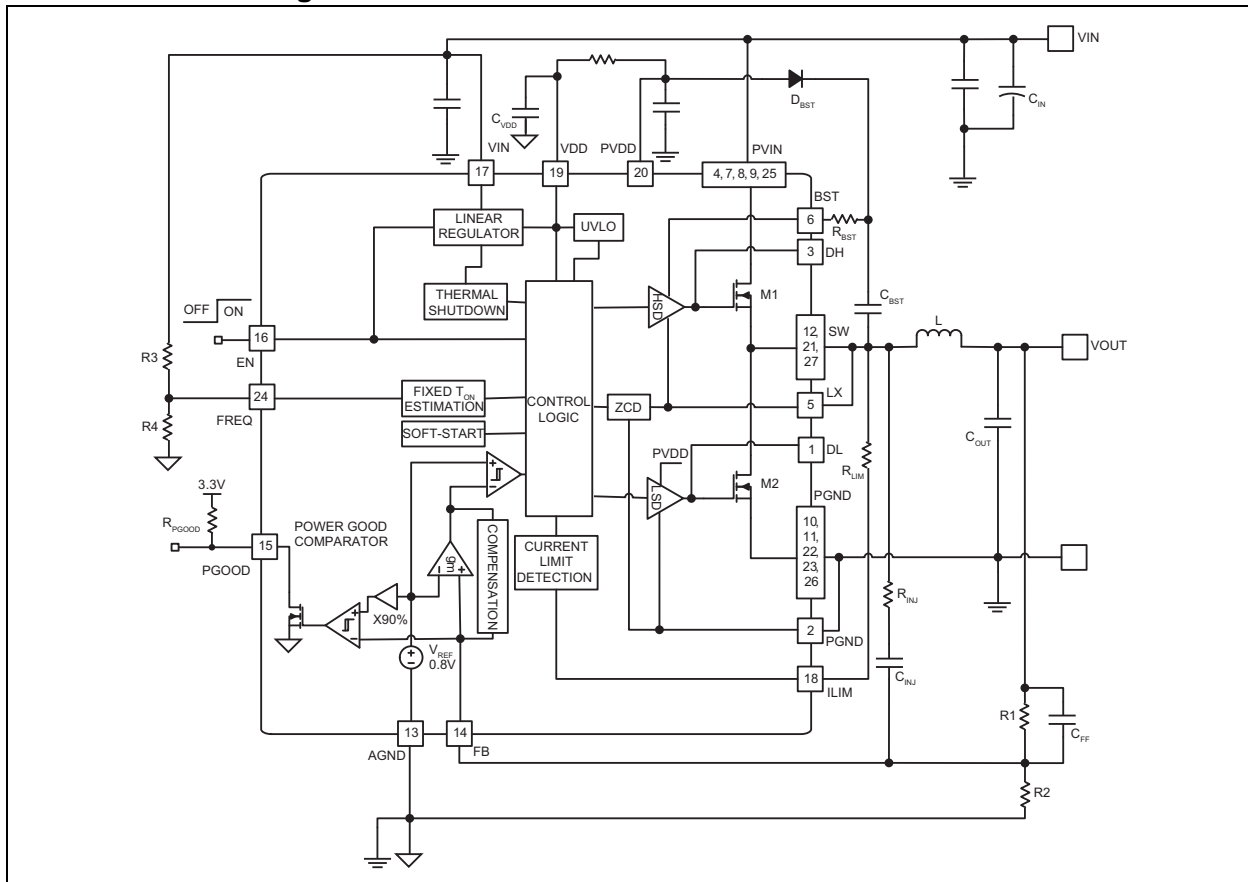


MIC28513

Typical Application Circuit



Functional Block Diagram



1.0 ELECTRICAL CHARACTERISTICS

Absolute Maximum Ratings †

PV_{IN} , V_{IN} to PGND.....	-0.3V to +50V
V_{DD} , P_{VDD} to PGND.....	-0.3V to +6V
V_{BST} to V_{SW} , V_{LX}	-0.3V to +6V
V_{BST} to PGND.....	-0.3V to ($V_{IN} + 6V$)
V_{SW} , V_{LX} to PGND.....	-0.3V to ($V_{IN} + 0.3V$)
V_{FREQ} , V_{ILIM} , V_{EN} to AGND.....	-0.3V to ($V_{IN} + 0.3V$)
V_{FB} , V_{PG} to AGND.....	-0.3V to ($V_{DD} + 0.3V$)
PGND to AGND.....	-0.3V to +0.3V
ESD Rating ⁽¹⁾ (HBM).....	1.5 kV
ESD Rating ⁽¹⁾ (MM).....	150V

Operating Ratings ‡

Supply Voltage (PV_{IN} , V_{IN}).....	+4.6V to +45V
Enable Input (V_{EN}).....	0V to V_{IN}
V_{SW} , V_{FREQ} , V_{ILIM}	0V to V_{IN}

† **Notice:** Stresses above those listed under “Absolute Maximum Ratings” may cause permanent damage to the device. This is a stress rating only and functional operation of the device at those or any other conditions above those indicated in the operational sections of this specification is not intended. Exposure to maximum rating conditions for extended periods may affect device reliability.

‡ **Notice:** The device is not guaranteed to function outside its operating ratings.

Note 1: Devices are ESD sensitive. Handling precautions are recommended. Human body model, 1.5 k Ω in series with 100 pF.

MIC28513

TABLE 1-1: ELECTRICAL CHARACTERISTICS

Electrical Characteristics: $V_{IN} = 12V$, $T_A = 25^\circ C$, unless noted. Bold values indicate $-40^\circ C \leq T_J \leq +125^\circ C$. (Note 1).					
Parameters	Min.	Typ.	Max.	Units	Conditions
Power Supply Input					
Input Voltage Range (PV_{IN} , V_{IN})	4.6	—	45	V	—
Quiescent Supply Current	—	0.4	0.75	mA	$V_{FB} = 1.5V$ (MIC28513-1)
	—	0.7	1.5		$V_{FB} = 1.5V$ (MIC28513-2)
Shutdown Supply Current	—	0.1	10	μA	SW unconnected, $V_{EN} = 0V$
V_{DD} Supply					
V_{DD} Output Voltage	4.8	5.2	5.4	V	$V_{IN} = 7V$ to $45V$, $I_{VDD} = 10$ mA
V_{DD} UVLO Threshold	3.8	4.2	4.6	V	V_{DD} rising
V_{DD} UVLO Hysteresis	—	400	—	mV	—
Load Regulation at 40 mA	0.6	2	4.0	%	—
Reference					
Feedback Reference Voltage	0.792	0.8	0.808	V	$25^\circ C$ ($\pm 1\%$)
	0.784	0.8	0.816		$-40^\circ C \leq T_J \leq +125^\circ C$ ($\pm 2\%$)
FB Bias Current	—	5	500	nA	$V_{FB} = 0.8V$
Enable Control					
EN Logic Level High	1.8	—	—	V	—
EN Logic Level Low	—	—	0.6		—
EN Hysteresis	—	200	—	mV	—
EN Bias Current	—	5	40	μA	$V_{EN} = 12V$
Oscillator					
Switching Frequency	450	680	800	kHz	$V_{FREQ} = V_{IN}$
	—	340	—		$V_{FREQ} = 50\% V_{IN}$
Maximum Duty Cycle	—	85	—	%	—
Minimum Duty Cycle	—	0	—		$V_{FB} > 0.8V$
Minimum Off-Time	110	200	270	ns	—
Internal MOSFET					
High-Side NMOS On-Resistance	—	37	—	m Ω	—
Low-Side NMOS On-Resistance	—	20	—		—
Short-Circuit Protection					
Current-Limit Threshold	-30	-14	0	mV	$V_{FB} = 0.79V$
Short-Circuit Threshold	-24	-7	8		$V_{FB} = 0V$
Current-Limit Source Current	50	70	90	μA	$V_{FB} = 0.79V$
Short-Circuit Source Current	25	36	43		$V_{FB} = 0V$

Note 1: Specification for packaged product only.

TABLE 1-1: ELECTRICAL CHARACTERISTICS (CONTINUED)

Electrical Characteristics: $V_{IN} = 12V$, $T_A = 25^\circ C$, unless noted. Bold values indicate $-40^\circ C \leq T_J \leq +125^\circ C$. (Note 1).					
Parameters	Min.	Typ.	Max.	Units	Conditions
Leakage					
SW, BST Leakage Current	—	—	50	μA	—
Power Good (PGOOD)					
PGOOD Threshold Voltage	85	90	95	% V_{OUT}	Sweep V_{FB} from low to high
PGOOD Hysteresis	—	6	—		Sweep V_{FB} from high to low
PGOOD Delay Time	—	100	—	μs	Sweep V_{FB} from low to high
PGOOD Low Voltage	—	70	200	mV	$V_{FB} < 90\% \times V_{NOM}$, $I_{PGOOD} = 1\text{ mA}$
Thermal Protection					
Overtemperature Shutdown	—	160	—	$^\circ C$	T_J Rising
Overtemperature Shutdown Hysteresis	—	15	—	$^\circ C$	—
Soft-Start					
Soft-Start Time	—	5	—	ms	—

Note 1: Specification for packaged product only.

MIC28513

TEMPERATURE SPECIFICATIONS

Parameters	Sym.	Min.	Typ.	Max.	Units	Conditions
Temperature Ranges						
Junction Operating Temperature	T_J	-40	—	+125	°C	Note 1
Storage Temperature Range	T_S	-65	—	+150	°C	—
Maximum Junction Temperature	T_J	—	—	+150	°C	—
Lead Temperature	—	—	—	+300	°C	Soldering, 10s
Package Thermal Resistances						
Thermal Resistance 3 mm x 4 mm FQFN-24LD	θ_{JA}	—	30	—	°C/W	—

Note 1: The maximum allowable power dissipation is a function of ambient temperature, the maximum allowable junction temperature and the thermal resistance from junction to air (i.e., T_A , T_J , θ_{JA}). Exceeding the maximum allowable power dissipation will cause the device operating junction temperature to exceed the maximum +125°C rating. Sustained junction temperatures above +125°C can impact the device reliability.

2.0 TYPICAL PERFORMANCE CURVES

Note: The graphs and tables provided following this note are a statistical summary based on a limited number of samples and are provided for informational purposes only. The performance characteristics listed herein are not tested or guaranteed. In some graphs or tables, the data presented may be outside the specified operating range (e.g., outside specified power supply range) and therefore outside the warranted range.

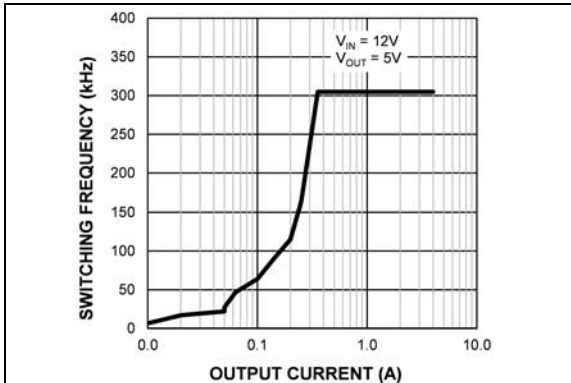


FIGURE 2-1: Switching Frequency vs. Output Current (MIC28513-1).

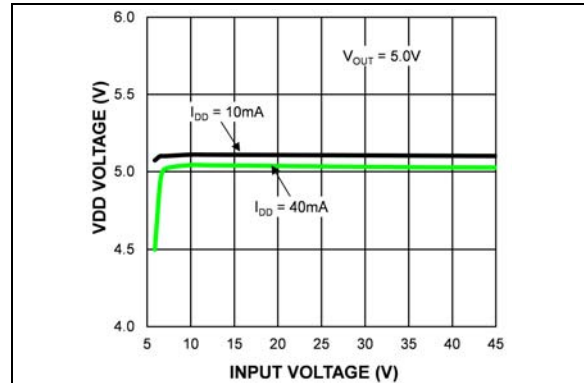


FIGURE 2-4: V_{DD} Voltage vs. Input Voltage.

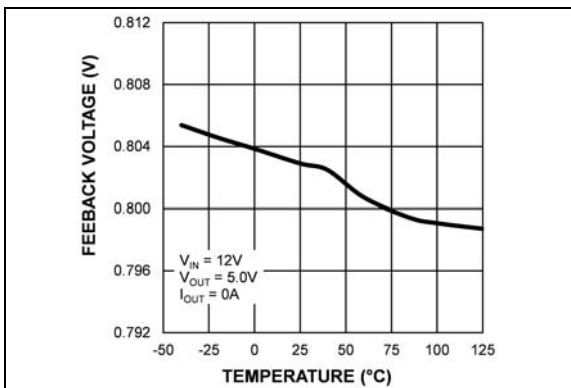


FIGURE 2-2: Feedback Voltage vs. Temperature (MIC28513-1).

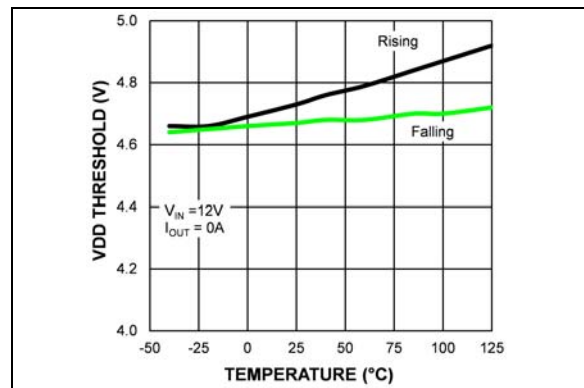


FIGURE 2-5: V_{DD} UVLO Threshold vs. Temperature (MIC28513-1).

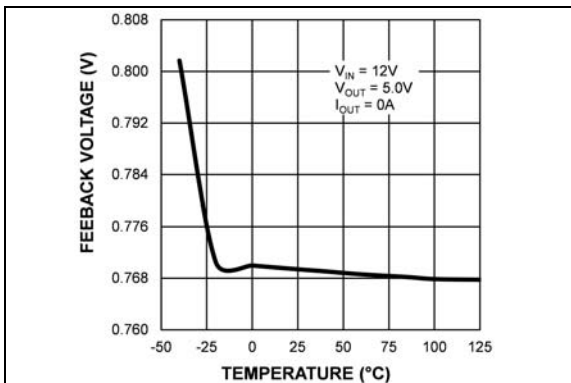


FIGURE 2-3: Feedback Voltage vs. Temperature (MIC28513-2).

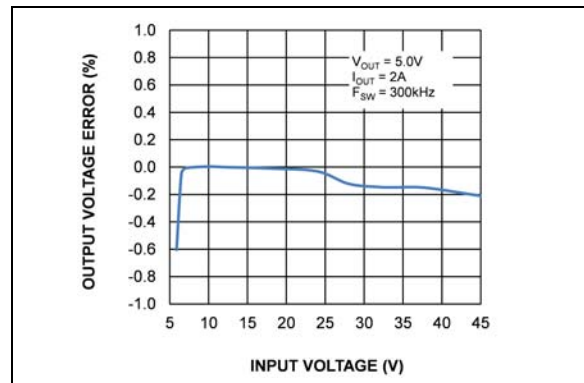


FIGURE 2-6: Line Regulation (V_{OUT} Error vs. V_{IN}).

MIC28513

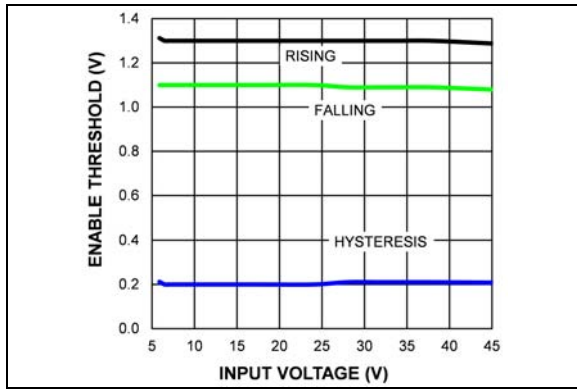


FIGURE 2-7: Enable Threshold vs. Input Voltage.

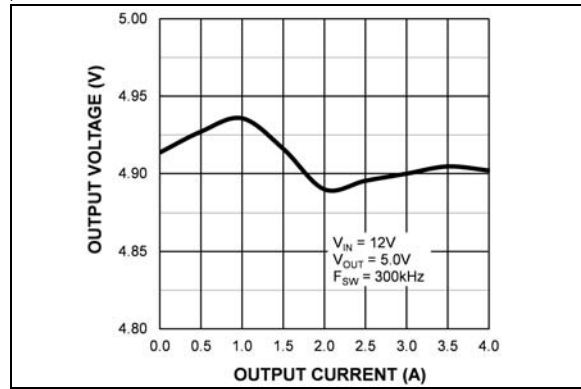


FIGURE 2-10: Output Voltage vs. Output Current (MIC28513-2).

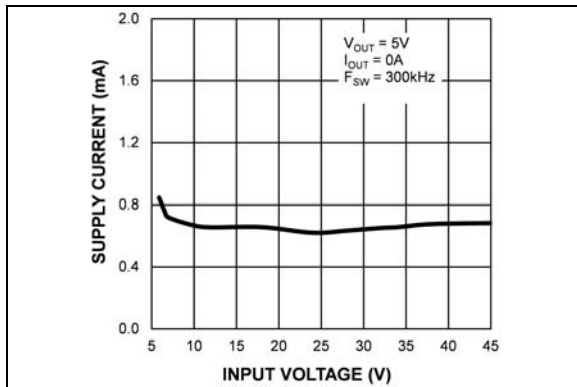


FIGURE 2-8: V_{IN} Operating Supply Current vs. Input Voltage (MIC28513-1).

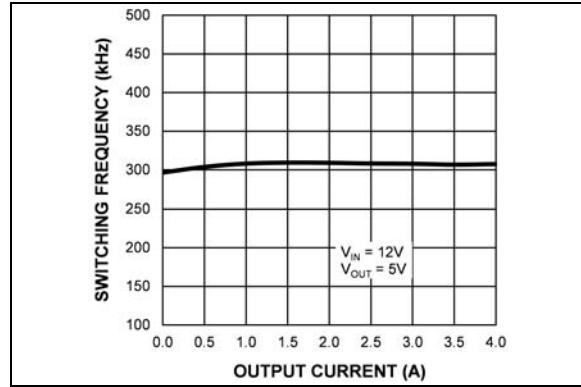


FIGURE 2-11: Switching Frequency vs. Output Current (MIC28513-2).

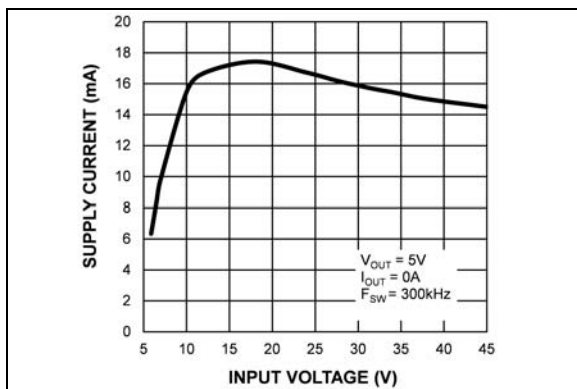


FIGURE 2-9: V_{IN} Operating Supply Current vs. Input Voltage (MIC28513-2).

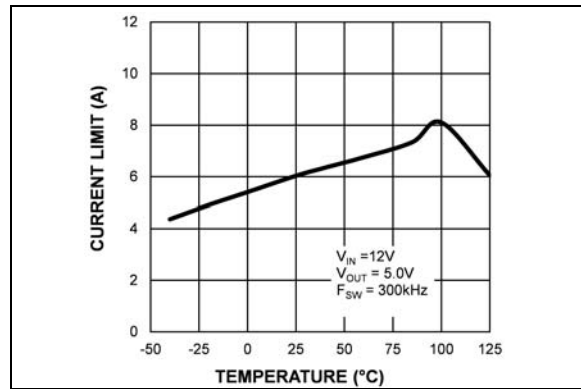


FIGURE 2-12: Output Peak Current Limit vs. Temperature (MIC28513-1).

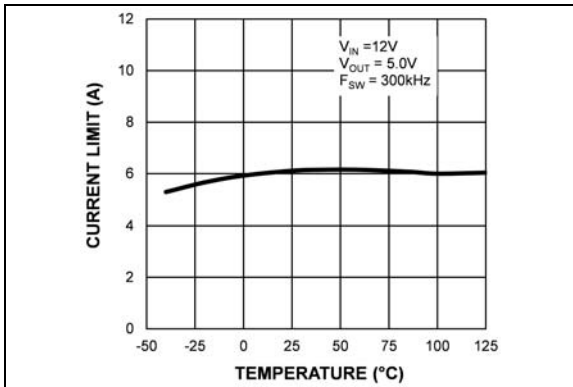


FIGURE 2-13: Output Peak Current Limit vs. Temperature (MIC28513-2).

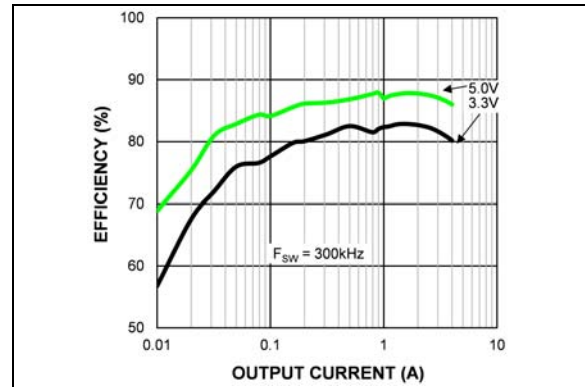


FIGURE 2-16: Efficiency ($V_{IN} = 36V$) vs. Output Current (MIC28513-1).

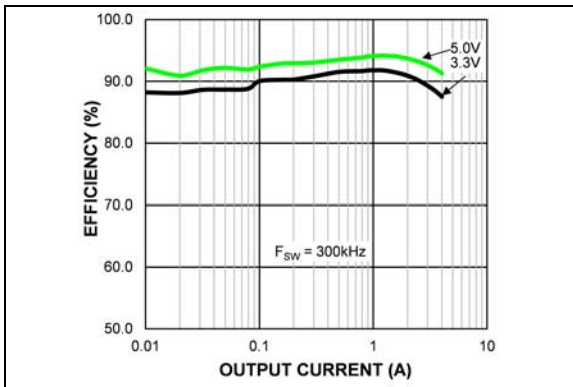


FIGURE 2-14: Efficiency ($V_{IN} = 12V$) vs. Output Current (MIC28513-1).

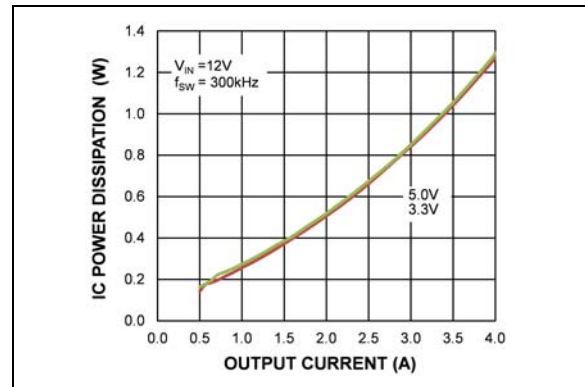


FIGURE 2-17: IC Power Dissipation vs. Output Current ($V_{IN} = 12V$).

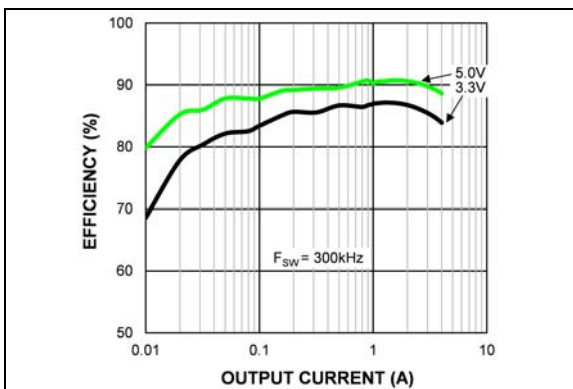


FIGURE 2-15: Efficiency ($V_{IN} = 24V$) vs. Output Current (MIC28513-1).

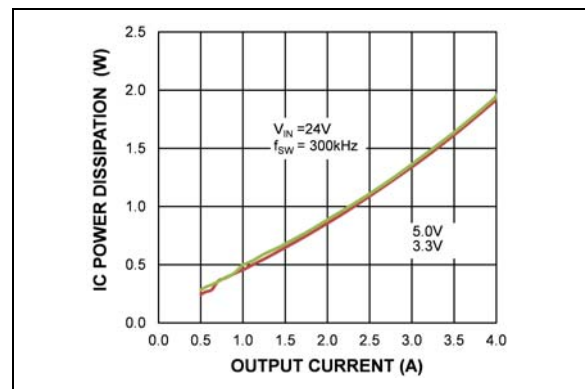


FIGURE 2-18: IC Power Dissipation vs. Output Current ($V_{IN} = 24V$).

MIC28513

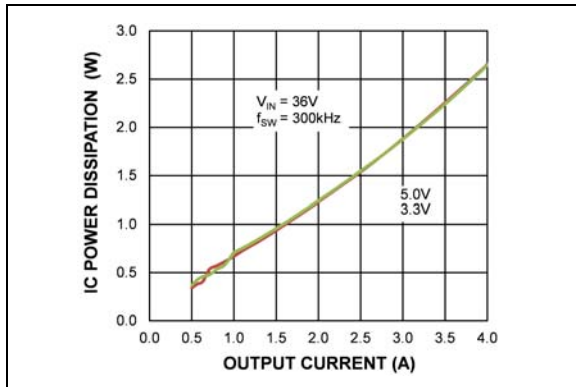


FIGURE 2-19: IC Power Dissipation vs. Output Current ($V_{IN} = 36V$).

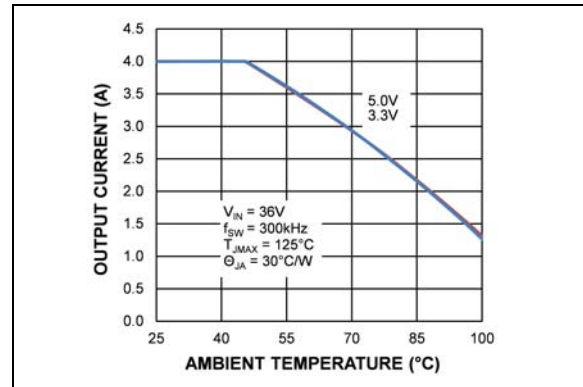


FIGURE 2-22: 36V Input Thermal Derating.

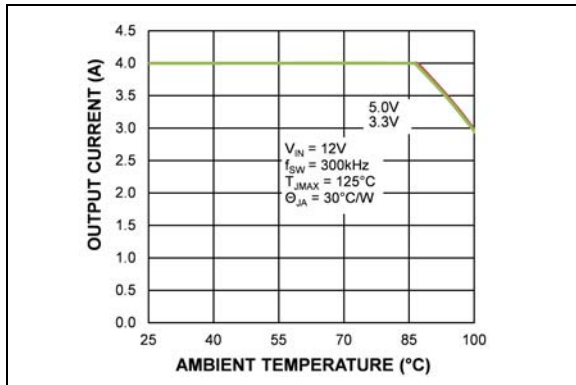


FIGURE 2-20: 12V Input Thermal Derating.

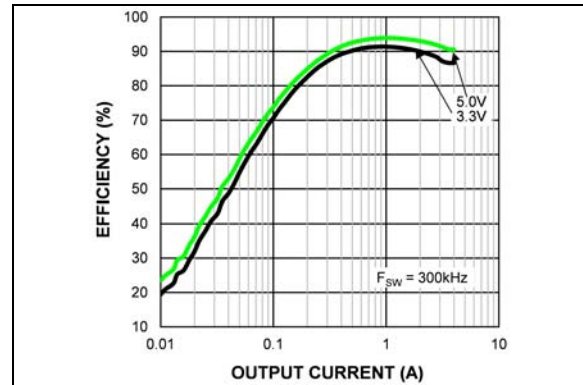


FIGURE 2-23: Efficiency ($V_{IN} = 12V$) vs. Output Current (MIC28513-2).

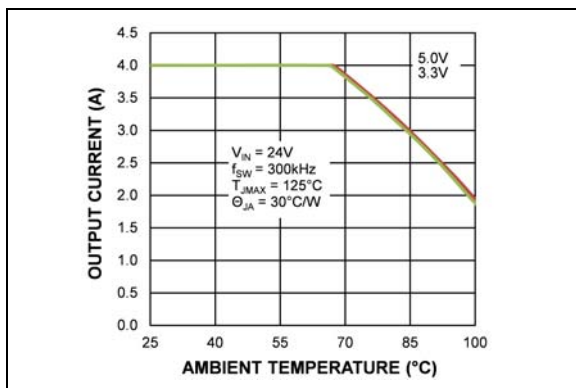


FIGURE 2-21: 24V Input Thermal Derating.

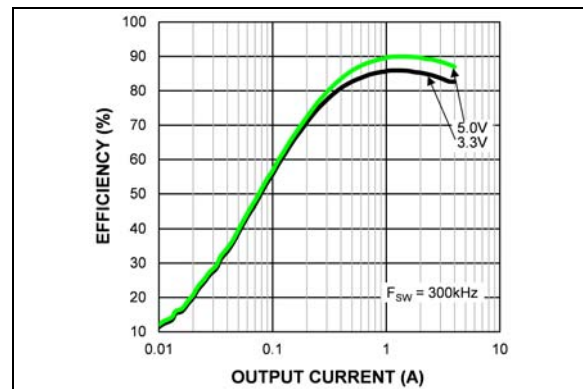


FIGURE 2-24: Efficiency ($V_{IN} = 24V$) vs. Output Current (MIC28513-2).

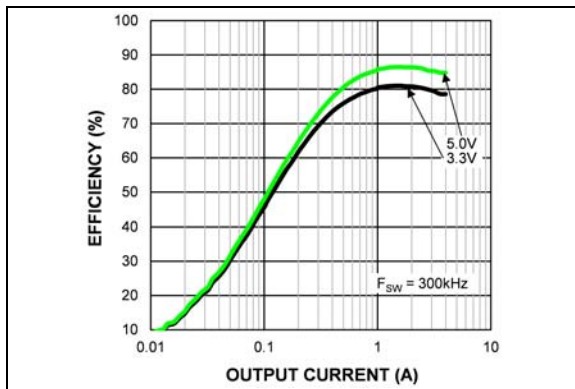


FIGURE 2-25: Efficiency ($V_{IN} = 36V$) vs. Output Current (MIC28513-2).

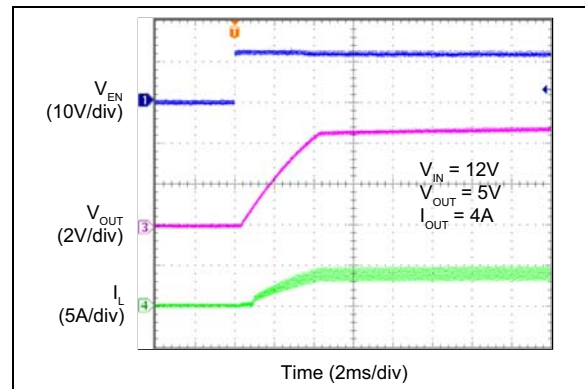


FIGURE 2-28: Enable Turn-On.

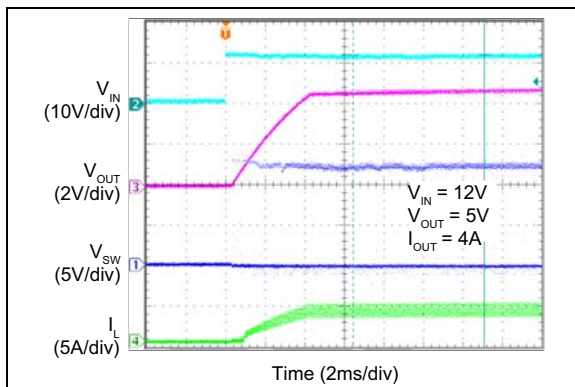


FIGURE 2-26: V_{IN} Turn-On.

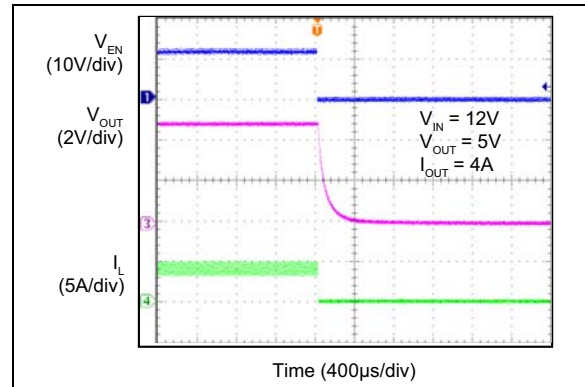


FIGURE 2-29: Enable Turn-Off.

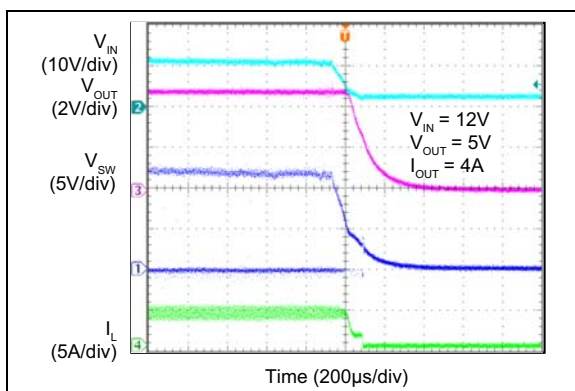


FIGURE 2-27: V_{IN} Turn-Off.

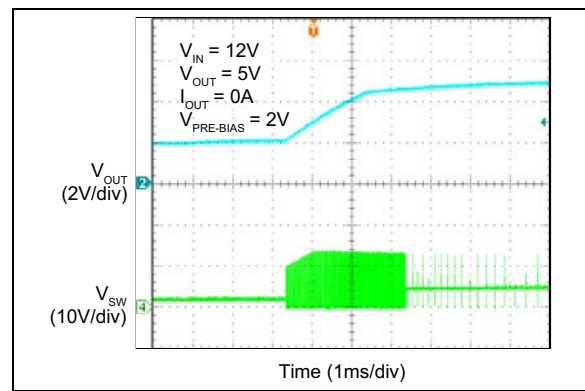


FIGURE 2-30: MIC28513-1 V_{IN} Start-Up with Pre-Biased Output ($I_{OUT} = 0A$).

MIC28513

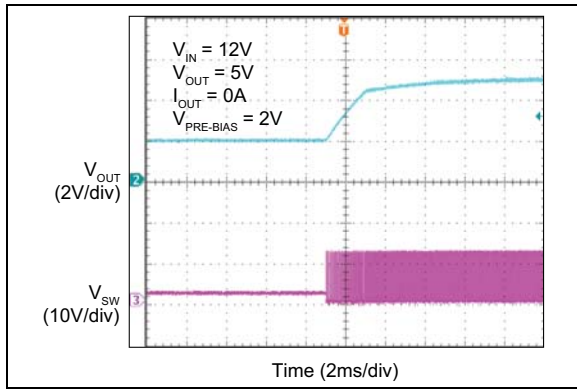


FIGURE 2-31: MIC28513-2 V_{IN} Start-Up with Pre-Biased Output ($I_{OUT} = 0A$).

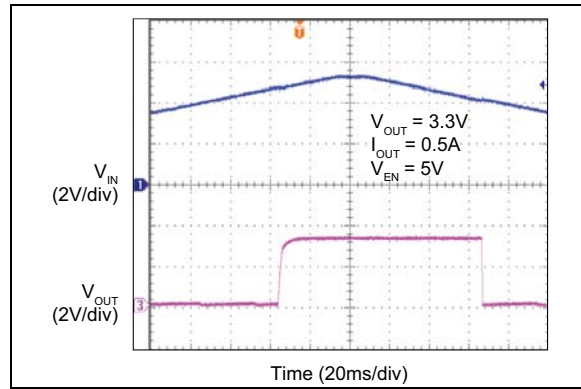


FIGURE 2-34: V_{IN} UVLO Thresholds.

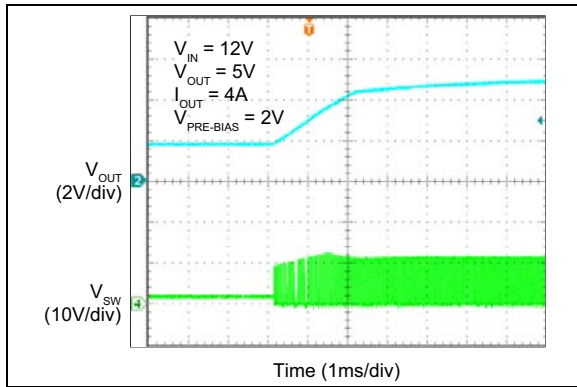


FIGURE 2-32: MIC28513-1 V_{IN} Start-Up with Pre-Biased Output ($I_{OUT} = 4A$).

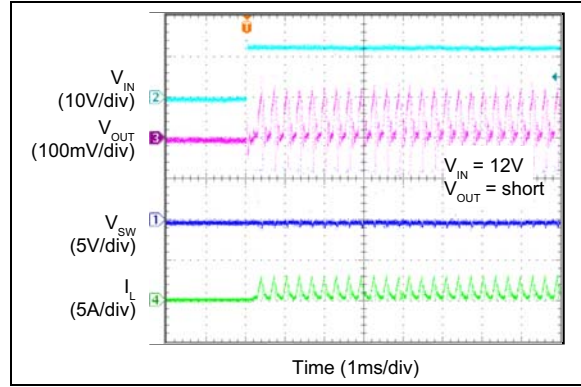


FIGURE 2-35: V_{IN} Turn-On Into Short-Circuit.

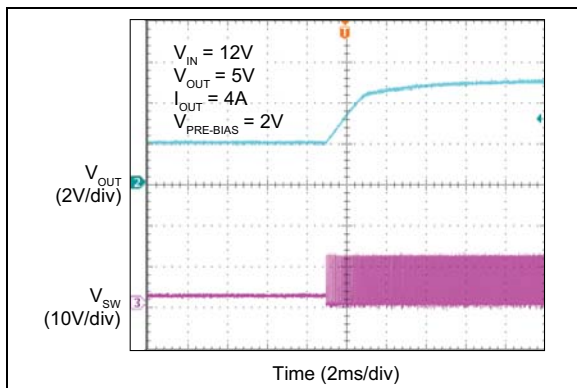


FIGURE 2-33: MIC28513-2 V_{IN} Start-Up with Pre-Biased Output ($I_{OUT} = 4A$).

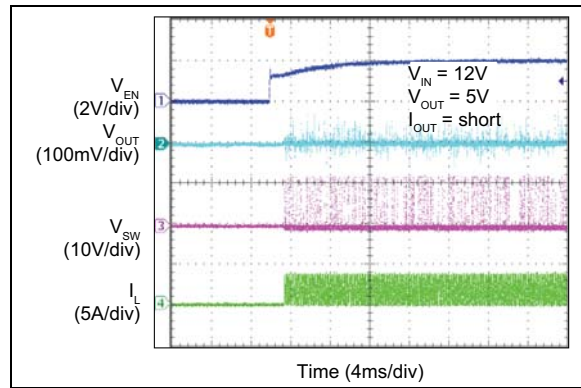


FIGURE 2-36: Enabled Into Short-Circuit.

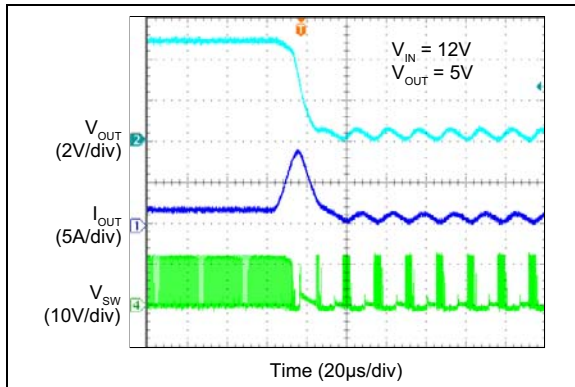


FIGURE 2-37: Overcurrent Protection.

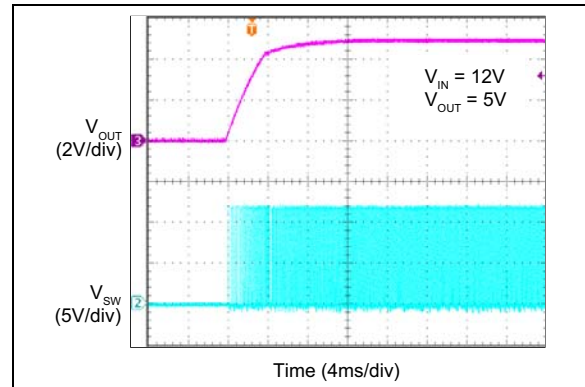


FIGURE 2-40: Output Recovery from Thermal Shutdown.

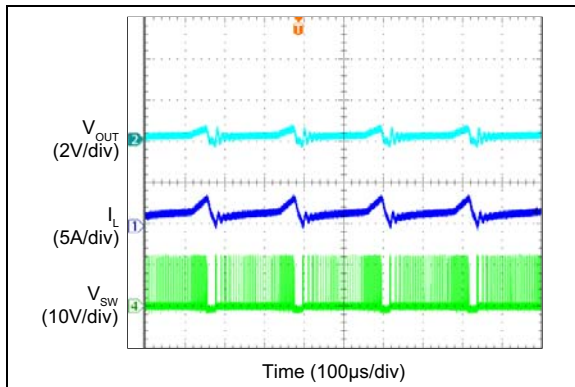


FIGURE 2-38: Overcurrent Protection Retry.

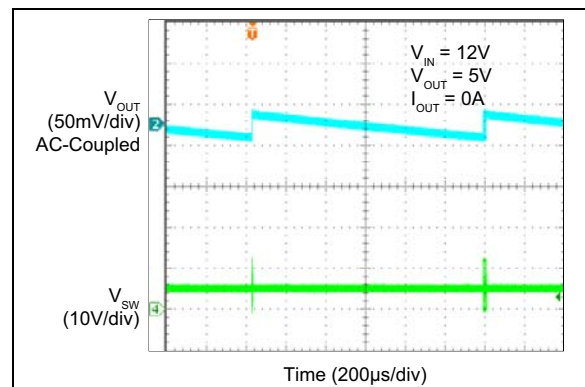


FIGURE 2-41: MIC28513-1 Switching Waveforms ($I_{OUT} = 0A$).

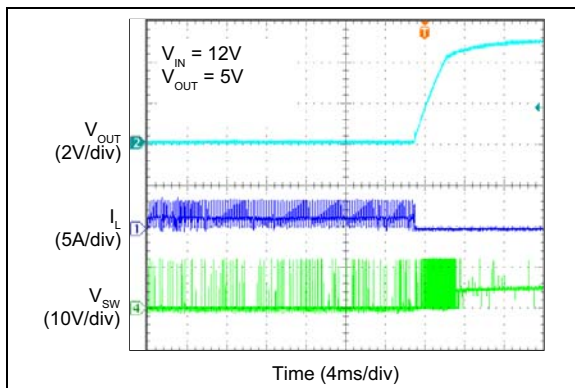


FIGURE 2-39: Output Recovery from Short-Circuit.

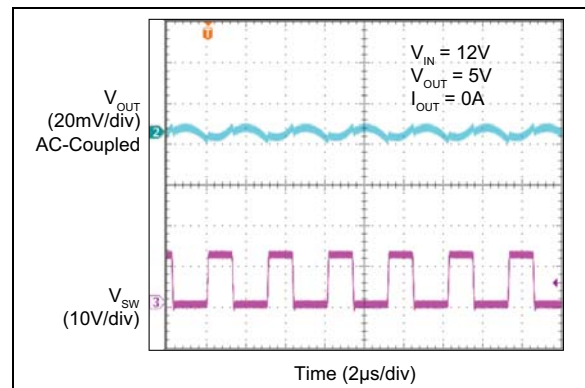


FIGURE 2-42: MIC28513-2 Switching Waveforms ($I_{OUT} = 0A$).

MIC28513

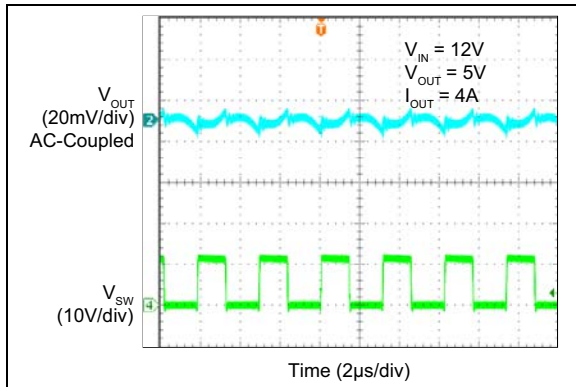


FIGURE 2-43: MIC28513-1 Switching Waveforms ($I_{OUT} = 4A$).

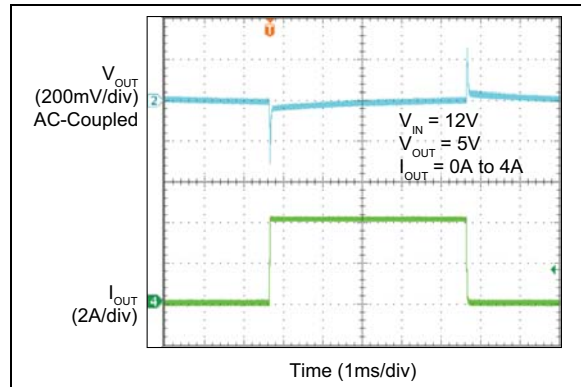


FIGURE 2-46: MIC28513-2 Load Transient Response (0A to 4A).

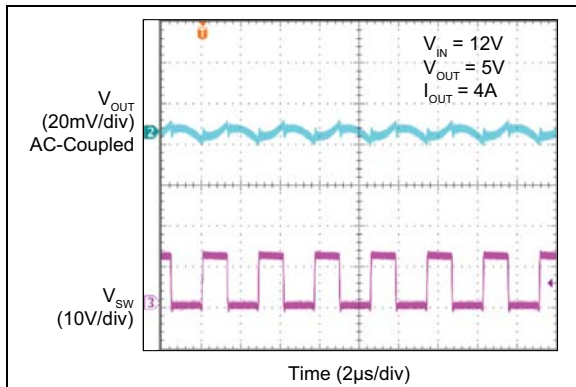


FIGURE 2-44: MIC28513-2 Switching Waveforms ($I_{OUT} = 4A$).

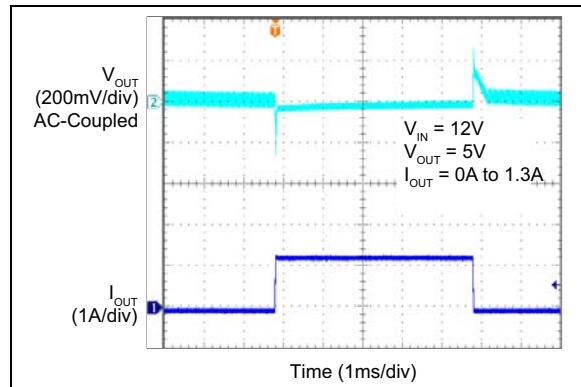


FIGURE 2-47: MIC28513-1 Load Transient Response (0A to 1.3A).

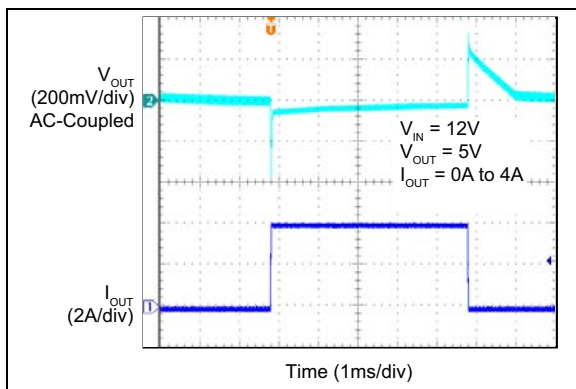


FIGURE 2-45: MIC28513-1 Load Transient Response (0A to 4A).

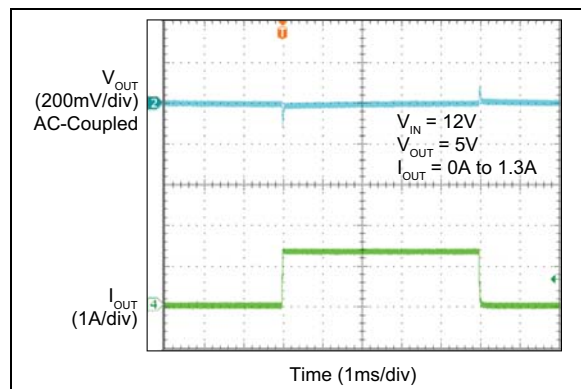


FIGURE 2-48: MIC28513-2 Load Transient Response (0A to 1.3A).

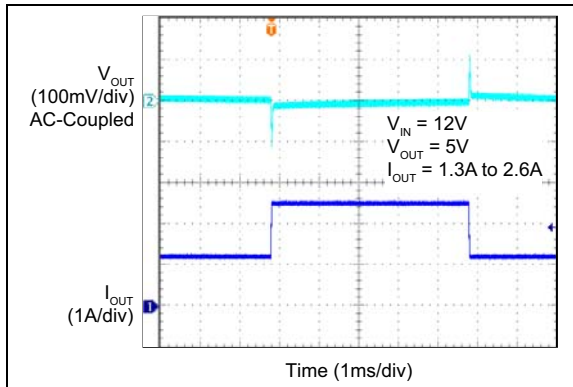


FIGURE 2-49: MIC28513-1 Load Transient Response (1.3A to 2.6A).

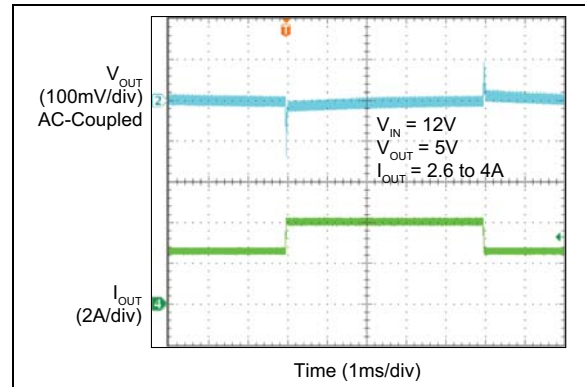


FIGURE 2-52: MIC28513-2 Load Transient Response (2.6A to 4A).

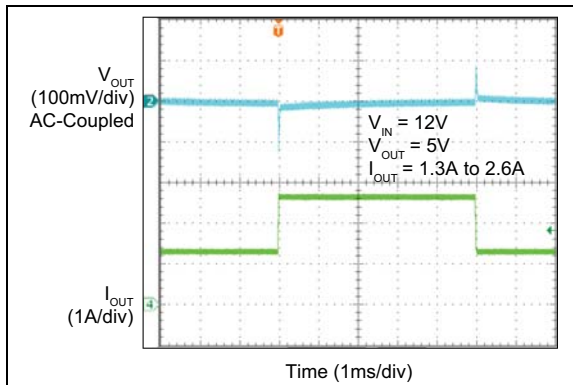


FIGURE 2-50: MIC28513-2 Load Transient Response (1.3A to 2.6A).

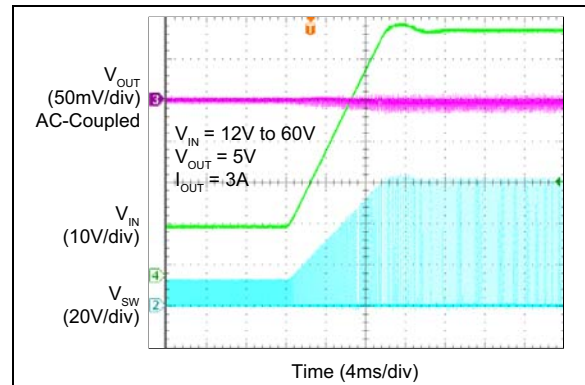


FIGURE 2-53: Line Transient Response.

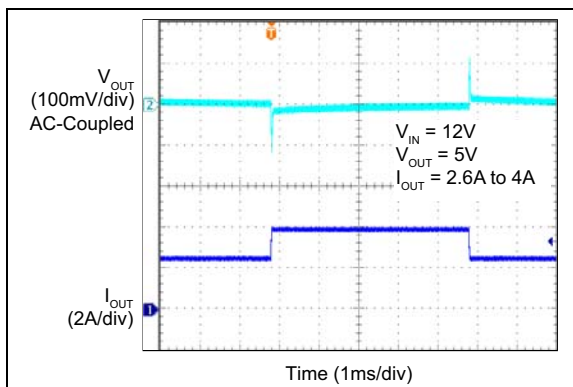


FIGURE 2-51: MIC28513-1 Load Transient Response (2.6A to 4A).

MIC28513

3.0 PIN DESCRIPTIONS

The descriptions of the pins are listed in [Table 3-1](#).

TABLE 3-1: PIN FUNCTION TABLE

Pin Number	Symbol	Description
1	DL	Low-Side Gate Drive. Internal low-side power MOSFET gate connection. This pin must be left unconnected or floating.
2	PGND	PGND is the return path for the low-side driver circuit. Connect to the source of low-side MOSFET (PGND, pins 10, 11, 22, 23, and 26) through a low-impedance path.
3	DH	High-Side Gate Drive. Internal high-side power MOSFET gate connection. This pin must be left unconnected or floating.
4, 7, 8, 9, 25 (25 is ePad)	PV _{IN}	Power Input Voltage. The PV _{IN} pins supply power to the internal power switch. Connect all PV _{IN} pins together and bypass locally with ceramic capacitors. The positive terminal of the input capacitor should be placed as close as possible to the PV _{IN} pins, the negative terminal of the input capacitor should be placed as close as possible to the PGND pins 10, 11, 22, 23, and 26.
5	LX	The LX pin is the return path for the high-side driver circuit. Connect the negative terminal of the bootstrap capacitor directly to this pin. Also connect this pin to the SW pins 12, 21, and 27, with a low-impedance path. The controller monitors voltages on this and PGND for zero current detection.
6	BST	Bootstrap Pin. This pin provides bootstrap supply for the high-side gate driver circuit. Connect a 0.1 μ F capacitor and an optional resistor in series from the LX (pin 5) to the BST pin.
10, 11, 22, 23, 26 (26 is ePad)	PGND	Power Ground. These pins are connected to the source of the low-side MOSFET. They are the return path for the step-down regulator power stage and should be tied together. The negative terminal of the input decoupling capacitor should be placed as close as possible to these pins.
12, 21, 27 (27 is ePad)	SW	Switch Node. The SW pins are the internal power switch outputs. These pins should be tied together and connected to the output inductor.
13	AGND	Analog Ground. The analog ground for V _{DD} and the control circuitry. The analog ground return path should be separate from the power ground (PGND) return path.
14	FB	Feedback Input. The FB pin sets the regulated output voltage relative to the internal reference. This pin is connected to a resistor divider from the regulated output such that the FB pin is at 0.8V when the output is at the desired voltage.
15	PGOOD	The power good output is an open drain output requiring an external pull-up resistor to external bias. This pin is a high impedance open circuit when the voltage at FB pin is higher than 90% of the feedback reference voltage (typically 0.8V).
16	EN	Enable Input. The EN pin enables the regulator. When the pin is pulled below the threshold, the regulator will shut down to an ultra-low current state. A precise threshold voltage allows the pin to operate as an accurate UVLO. Do not tie EN to V _{DD} .
17	V _{IN}	Supply voltage for the internal LDO. The V _{IN} operating voltage range is from 4.6V to 45V. A ceramic capacitor from V _{IN} to AGND is required for decoupling. The decoupling capacitor should be placed as close as possible to the supply pin.
18	I _{LIM}	Current Limit Setting. Connect a resistor from this pin to the SW pin node to allow for accurate current limit sensing programming of the internal low-side power MOSFET.
19	V _{DD}	Internal +5V Linear Regulator: V _{DD} is the internal supply bus for the IC. Connect to an external 1 μ F bypass capacitor. When V _{IN} is <5.5V, this regulator operates in drop-out mode. Connect V _{DD} to V _{IN} .
20	PV _{DD}	A 5V supply input for the low-side N-channel MOSFET driver circuit, which can be tied to V _{DD} externally. A 1 μ F ceramic capacitor from PV _{DD} to PGND is recommended for decoupling.
24	FREQ	Switching Frequency Adjust pin. Connect this pin to V _{IN} to operate at 680 kHz. Place a resistor divider network from V _{IN} to the FREQ pin to program the switching frequency.

4.0 FUNCTIONAL DESCRIPTION

The MIC28513 is an adaptive on-time synchronous buck regulator with integrated high-side and low-side MOSFETs suitable for high-input voltage to low-output voltage conversion applications. It is designed to operate over a wide input voltage range, from 4.6V to 45V, which is suitable for automotive and industrial applications. The output is adjustable with an external resistive divider. An adaptive on-time control scheme is employed to produce a constant switching frequency in continuous-conduction mode and reduced switching frequency in discontinuous-operation mode, improving light-load efficiency. Overcurrent protection is implemented by sensing the low-side MOSFET's $R_{DS(ON)}$. The device features internal soft-start, enable, UVLO, and thermal shutdown.

4.1 Theory of Operation

As illustrated in the [Functional Block Diagram](#), the output voltage is sensed by the feedback (FB) pin via voltage divider resistors R1 and R2, and compared to a 0.8V reference voltage V_{REF} at the error comparator through a low-gain transconductance (g_M) amplifier. If the feedback voltage decreases and the amplifier output is below 0.8V, then the error comparator will trigger the control logic and generate an ON-time period. The ON-time period length is predetermined by the fixed t_{ON} estimator circuitry:

EQUATION 4-1:

$$t_{ON(ESTIMATED)} = \frac{V_{OUT}}{V_{IN} \times f_{SW}}$$

Where:

V_{OUT}	Output Voltage
V_{IN}	Power Stage Input Voltage
f_{SW}	Switching Frequency

At the end of the ON-time period, the internal high-side driver turns off the high-side MOSFET and the low-side driver turns on the low-side MOSFET. The OFF-time period length depends upon the feedback voltage in most cases. When the feedback voltage decreases and the output of the g_M amplifier is below 0.8V, then the ON-time period is triggered and the OFF-time period ends. If the OFF-time period determined by the feedback voltage is less than the minimum OFF-time $t_{OFF(MIN)}$, which is about 200 ns (typical), the MIC28513 control logic will apply the $t_{OFF(MIN)}$ instead. The $t_{OFF(MIN)}$ is required to maintain enough energy in the boost capacitor (C_{BST}) to drive the high-side MOSFET.

The maximum duty cycle is obtained from [Equation 4-2](#).

EQUATION 4-2:

$$D_{MAX} = 1 - t_{OFF(MIN)} \times f_{SW}$$

It is not recommended to use MIC28513 with an OFF-time close to $t_{OFF(MIN)}$ during steady-state operation.

The adaptive ON-time control scheme results in a constant switching frequency in the MIC28513. The actual ON-time and resulting switching frequency will vary with the different rising and falling times of the internal MOSFETs. Also, the minimum t_{ON} results in a lower switching frequency in high V_{IN} to V_{OUT} applications. During load transients, the switching frequency is changed due to the varying OFF-time.

[Figure 4-1](#) shows the allowable range of the output voltage versus the input voltage. The minimum output voltage is 0.8V which is limited by the reference voltage. The maximum output voltage is 24V which is limited by the internal circuitry.

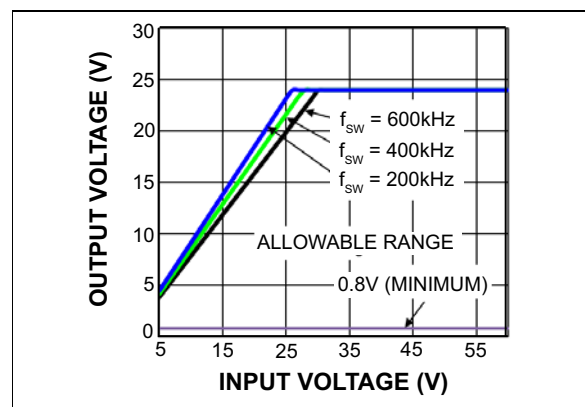


FIGURE 4-1: Allowable Output Voltage Range vs. Input Voltage.

To illustrate the control loop operation, both the steady-state and load transient scenarios will be analyzed.

[Figure 4-2](#) shows the MIC28513 control loop timing during steady-state operation. During steady-state, the g_M amplifier senses the feedback voltage ripple, which is proportional to the output voltage ripple and the inductor current ripple, to trigger the ON-time period. The ON-time is predetermined by the t_{ON} estimator. The termination of the OFF-time is controlled by the feedback voltage. At the valley of the feedback voltage ripple, which occurs when V_{FB} falls below V_{REF} , the OFF period ends and the next ON-time period is triggered through the control logic circuitry.

MIC28513

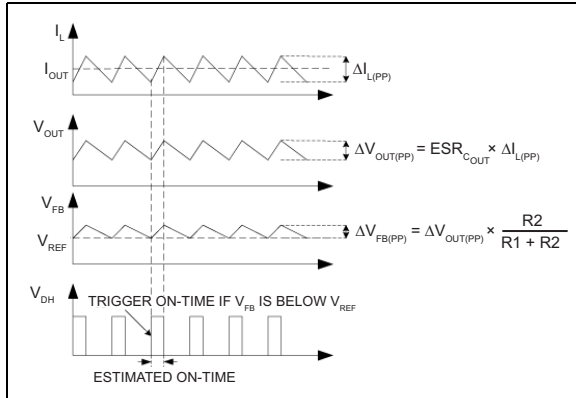


FIGURE 4-2: MIC28513 Control Loop Timing.

Figure 4-3 shows the operation of the MIC28513 during a load transient. The output voltage drops due to the sudden load increase, which causes the V_{FB} to be less than V_{REF} . This will cause the error comparator to trigger an ON-time period. At the end of the ON-time period, a minimum OFF-time $t_{OFF(MIN)}$ is generated to charge C_{BST} because the feedback voltage is still below V_{REF} . Then, the next ON-time period is triggered due to the low feedback voltage. Therefore, the switching frequency changes during the load transient, but returns to the nominal fixed frequency once the output has stabilized at the new load current level. With the varying duty cycle and switching frequency, the output recovery time is fast and the output voltage deviation is small in MIC28513 converter.

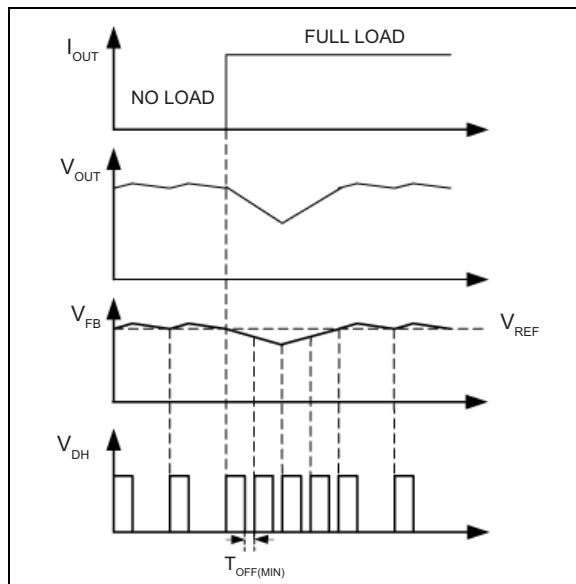


FIGURE 4-3: MIC28513 Load Transient Response.

Unlike true current-mode control, the MIC28513 uses the output voltage ripple to trigger an ON-time period. The output voltage ripple is proportional to the inductor

current ripple if the ESR of the output capacitor is large enough. The MIC28513 control loop has the advantage of eliminating the need for slope compensation.

In order to meet the stability requirements, the MIC28513 feedback voltage ripple should be in phase with the inductor current ripple and large enough to be sensed by the g_M amplifier and the error comparator. The recommended feedback voltage ripple is 20 mV ~ 100 mV.

If a low-ESR output capacitor is selected, then the feedback voltage ripple may be too small to be sensed by the g_M amplifier and the error comparator. Also, if the ESR of the output capacitor is very low, the output voltage ripple and the feedback voltage ripple are not necessarily in phase with the inductor current ripple. In these cases, ripple injection is required to ensure proper operation. Please refer to the [Ripple Injection](#) subsection for more details about the ripple injection technique.

4.2 Discontinuous Mode (MIC28513-1 Only)

In continuous mode, the inductor current is always greater than zero; however, at light loads the MIC28513-1 is able to force the inductor current to operate in discontinuous mode. Discontinuous mode occurs when the inductor current falls to zero, as indicated by trace (I_L) shown in Figure 4-4. During this period, the efficiency is optimized by shutting down all the non-essential circuits and minimizing the supply current. The MIC28513-1 wakes up and turns on the high-side MOSFET when the feedback voltage V_{FB} drops below 0.8V.

The MIC28513-1 has a zero crossing comparator that monitors the inductor current by sensing the voltage drop across the low-side MOSFET during its ON-time. If the $V_{FB} > 0.8V$ and the inductor current goes slightly negative, then the MIC28513-1 automatically powers down most of the IC circuitry and goes into a low-power mode.

Once the MIC28513-1 goes into discontinuous mode, both DH and DL are low, which turns off the high-side and low-side MOSFETs. The load current is supplied by the output capacitors and V_{OUT} drops. If the drop of V_{OUT} causes V_{FB} to go below V_{REF} , then all the circuits will wake up into normal continuous mode. First, the bias currents of most circuits reduced during the discontinuous mode are restored, and then a t_{ON} pulse is triggered before the drivers are turned on to avoid any possible glitches. Finally, the high-side driver is turned on. Figure 4-4 shows the control loop timing in discontinuous mode.

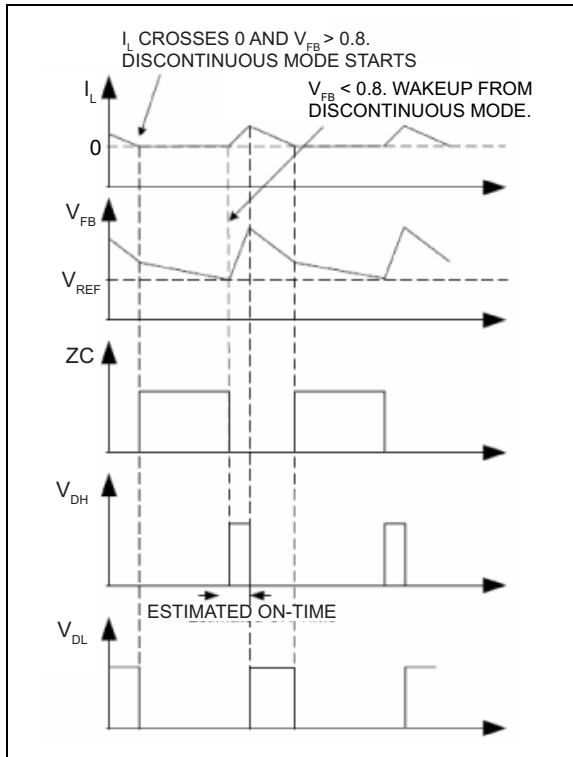


FIGURE 4-4: MIC28513-1 Control Loop Timing (Discontinuous Mode).

During discontinuous mode, the bias current of most circuits are reduced. As a result, the total power supply current during discontinuous mode is only about 450 μA , allowing the MIC28513-1 to achieve high efficiency in light load applications.

4.3 V_{DD} Regulator

The MIC28513 provides a 5V regulated V_{DD} to bias internal circuitry for V_{IN} ranging from 5.5V to 45V. When V_{IN} is less than 5.5V, V_{DD} should be tied to V_{IN} pins to bypass the internal linear regulator.

4.4 Soft-Start

Soft-start reduces the power supply inrush current at startup by controlling the output voltage rise time while the output capacitor charges.

The MIC28513 implements an internal digital soft-start by ramping up the 0.8V reference voltage (V_{REF}) from 0 to 100% in about 5 ms with 9.7 mV steps. This controls the output voltage rate of rise at turn on, minimizing inrush current and eliminating output voltage overshoot. Once the soft-start cycle ends, the related circuitry is disabled to reduce current consumption.

4.5 Current Limit

The MIC28513 uses the $R_{DS(ON)}$ of the internal low-side power MOSFET to sense overcurrent conditions. In each switching cycle, the inductor current is sensed by monitoring the low-side MOSFET during its ON period. The sensed voltage, $V_{(ILIM)}$, is compared with the power ground (PGND) after a blanking time of 150 ns.

The voltage drop of the resistor R_{ILIM} is compared with the low-side MOSFET voltage drop to set the overcurrent trip level. The small capacitor connected from the I_{LIM} pin to PGND can be added to filter the switching node ringing, allowing a better short limit measurement. The time constant created by R_{ILIM} and the filter capacitor should be much less than the minimum off time.

The overcurrent limit can be programmed by using [Equation 4-3](#):

EQUATION 4-3:

$$R_{ILIM} = \frac{(I_{CLIM} + 0.5 \times \Delta I_{L(PP)}) \times R_{DS(ON)} + V_{CL}}{I_{CL}}$$

Where:

I_{CLIM}	Desired Output Current Limit
$\Delta I_{L(PP)}$	Inductor Current Peak-to-Peak Use Equation 4-4 to calculate the inductor ripple current
$R_{DS(ON)}$	On-Resistance of Low-Side MOSFET
V_{CL}	Current-limit threshold. 14 mV (typical).
I_{CL}	Current-limit source current. 70 μA (typical).

The peak-to-peak inductor current ripple is calculated with [Equation 4-4](#).

EQUATION 4-4:

$$\Delta I_{L(PP)} = \frac{V_{OUT} \times (V_{IN(MAX)} - V_{OUT})}{V_{IN(MAX)} \times f_{SW} \times L}$$

The MOSFET $R_{DS(ON)}$ varies 30% to 40% with temperature; therefore, it is recommended to use the $R_{DS(ON)}$ at maximum junction temperature with a 20% margin to calculate R_{ILIM} in [Equation 4-3](#).

In case of hard short, the current-limit threshold is folded down to allow an indefinite hard short on the output without any destructive effect. It is mandatory to make sure that the inductor current used to charge the output capacitor during soft-start is under the folded short limit; otherwise the supply will go into hiccup mode and may not be finishing the soft-start successfully.

MIC28513

When operating at higher input voltages, it is recommended to look at safe operating area (SOA) curves while selecting output current limit threshold. SOA curves for MIC28513 are given in [Figure 2-21](#) and [Figure 2-22](#).

4.6 Output Current Thermal Derating

MIC28513 is packaged in a 3 mm x 4 mm FQFN package. The output current derates with temperature when operating with higher input voltages at higher temperature as shown in [Figure 2-21](#) and [Figure 2-22](#).

4.7 Power Good (PGOOD)

The power good (PGOOD) pin is an open-drain output that indicates logic-high when the output is nominally 90% of its steady-state voltage.

4.8 MOSFET Gate Drive

The [Functional Block Diagram](#) shows a bootstrap circuit, consisting of D_{BST} , C_{BST} , and R_{BST} . This circuit supplies energy to the high-side drive circuit. Capacitor C_{BST} is charged, while the low-side MOSFET is on, and the voltage on the SW pin is approximately 0V. When the high-side MOSFET driver is turned on, energy from C_{BST} is used to turn the MOSFET on. As the high-side MOSFET turns on, the voltage on the SW pin increases to approximately V_{IN} . Diode D_{BST} is reverse-biased and C_{BST} floats high while continuing to bias the high-side gate driver. The bias current of the high-side driver is less than 10 mA, so a 0.1 μ F to 1 μ F capacitor is sufficient to hold the gate voltage with minimal droop for the power stroke (high-side switching) cycle, i.e. $\Delta BST = 10 \text{ mA} \times 1.25 \mu\text{s} / 0.1 \mu\text{F} = 125 \text{ mV}$. When the low-side MOSFET is turned back on, C_{BST} is then recharged through the boost diode. A 30 Ω resistor R_{BST} , which is in series with the C_{BST} capacitor, is required to slow down the turn-on time of the high-side N-channel MOSFET.

5.0 APPLICATION INFORMATION

5.1 Output Voltage Setting Components

The MIC28513 requires two resistors to set the output voltage as shown in Figure 5-1.

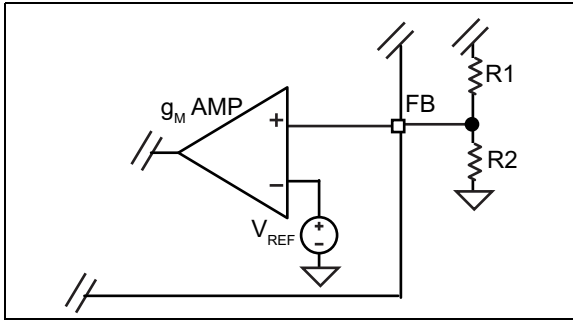


FIGURE 5-1: Voltage Divider Configuration.

The output voltage is determined by Equation 5-1.

EQUATION 5-1:

$$V_{OUT} = V_{FB} \times \left(1 + \frac{R1}{R2}\right)$$

Where:

$$V_{FB} = 0.8V$$

A typical value of R1 used on the standard evaluation board is 10 kΩ. If R1 is too large, it may allow noise to be introduced into the voltage feedback loop. If R1 is too small in value, it will decrease the efficiency of the buck regulator, especially at light loads. Once R1 is selected, R2 can be calculated using Equation 5-2:

EQUATION 5-2:

$$R2 = \frac{V_{FB} \times R1}{V_{OUT} - V_{FB}}$$

5.2 Setting the Switching Frequency

The MIC28513 switching frequency can be adjusted by changing the resistor divider network from V_{IN}.

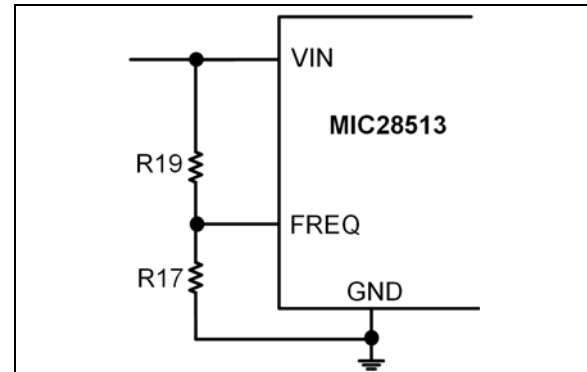


FIGURE 5-2: Switching Frequency Adjustment.

Equation 5-3 gives the estimated switching frequency.

EQUATION 5-3:

$$f_{sw} = f_0 \times \left(\frac{R17}{R17 + R19}\right)$$

Where:

f_0 Switching frequency when R17 is open; typically 600 kHz.

Figure 5-3 shows the switching frequency versus the resistor R17 when R19 = 100 kΩ.

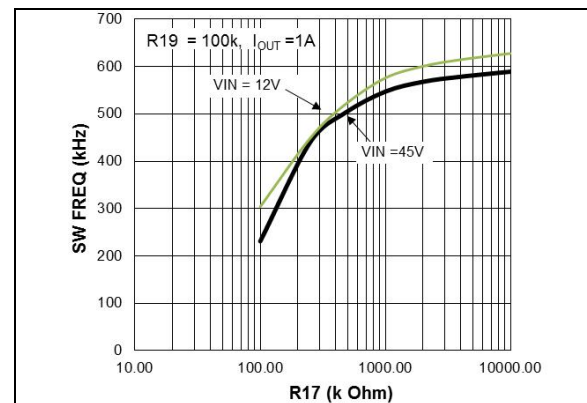


FIGURE 5-3: Switching Frequency vs. R17.

5.3 Inductor Selection

Values for inductance, peak, and RMS currents are required to select the output inductor. The input and output voltages and the inductance value determine the peak-to-peak inductor ripple current. Generally, higher inductance values are used with higher input voltages. Larger peak-to-peak ripple currents will increase the power dissipation in the inductor and

MIC28513

MOSFETs. Larger output ripple currents will also require more output capacitance to smooth out the larger ripple current. Smaller peak-to-peak ripple currents require a larger inductance value and therefore a larger and more expensive inductor. A good compromise between size, loss and cost is to set the inductor ripple current to be equal to 20% of the maximum output current. The inductance value is calculated by:

EQUATION 5-4:

$$L = \frac{V_{OUT} \times (V_{IN(MAX)} - V_{OUT})}{V_{IN(MAX)} \times \Delta I_{L(PP)} \times f_{SW}}$$

Where:

f_{SW}	Switching Frequency
$\Delta I_{L(PP)}$	The peak-to-peak inductor current ripple; typically 20% of the maximum output current

In continuous conduction mode, the peak inductor current is equal to the average output current plus one half of the peak-to-peak inductor current ripple.

EQUATION 5-5:

$$I_{L(RMS)} = I_{OUT} + 0.5 \times \Delta I_{L(PP)}$$

The RMS inductor current is used to calculate the I^2R losses in the inductor.

EQUATION 5-6:

$$I_{L(RMS)} = \sqrt{I_{OUT(MAX)}^2 + \frac{\Delta I_{L(PP)}^2}{12}}$$

Maximizing efficiency requires the proper selection of core material and minimizing the winding resistance. The high-frequency operation of the MIC28513 requires the use of ferrite materials for all but the most cost-sensitive applications. Lower cost iron powder cores may be used but the increase in core loss will reduce the efficiency of the buck regulator. This is especially noticeable at low output power. The winding resistance decreases efficiency at the higher output current levels.

The winding resistance must be minimized although this usually comes at the expense of a larger inductor. The power dissipated in the inductor is equal to the sum of the core and copper losses. At higher output loads, the core losses are usually insignificant and can be

ignored. At lower output currents, the core losses can be a significant contributor. Core loss information is usually available from the magnetics vendor. Copper loss in the inductor is calculated by [Equation 5-7](#):

EQUATION 5-7:

$$P_{L(CU)} = I_{L(RMS)}^2 \times DCR$$

The resistance of the copper wire, DCR, increases with the temperature. The value of the winding resistance used should be at the operating temperature.

EQUATION 5-8:

$$DCR_{(HT)} = DCR_{(20C)} \times (1 + 0.0042 \times [T_H - T_{20C}])$$

Where:

T_H	Temperature of wire under full load
T_{20C}	Room temperature
$DCR_{(20C)}$	Room temperature winding resistance (usually specified by the manufacturer)

5.4 Output Capacitor Selection

The type of the output capacitor is usually determined by its equivalent series resistance (ESR). Voltage and RMS current capability are also important factors in selecting an output capacitor. Recommended capacitor types are ceramic, tantalum, low-ESR aluminum electrolytic, OS-CON and POSCAP. For high ESR electrolytic capacitors, ESR is the main cause of the output ripple. The output capacitor ESR also affects the control loop from a stability point of view. For a low ESR ceramic output capacitor, ripple is dominated by the reactive impedance. The maximum value of ESR is calculated by [Equation 5-9](#).

EQUATION 5-9:

$$ESR_{C_{OUT}} \leq \frac{\Delta V_{OUT(PP)}}{\Delta I_{L(PP)}}$$

Where:

$\Delta V_{OUT(PP)}$	Peak-to-Peak Output Voltage Ripple
$\Delta I_{L(PP)}$	Peak-to-Peak Inductor Current Ripple

The total output ripple is a combination of voltage ripples caused by the ESR and output capacitance. The total ripple is calculated by [Equation 5-10](#).

EQUATION 5-10:

$$\Delta V_{OUT(PP)} = \sqrt{\left(\frac{\Delta I_{L(PP)}}{C_{OUT} \times f_{SW} \times 8}\right)^2 + (\Delta I_{L(PP)} \times ESR_{COUT})^2}$$

Where:

C_{OUT} Output Capacitance Value
 f_{SW} Switching Frequency

As described in the [Theory of Operation](#) subsection of the [Functional Description](#), the MIC28513 requires at least 20 mV peak-to-peak ripple at the FB pin for the g_M amplifier and the error comparator to operate properly. Also, the ripple on FB pin should be in phase with the inductor current. Therefore, the output voltage ripple caused by the output capacitors value should be much smaller than the ripple caused by the output capacitor ESR. If low-ESR capacitors, such as ceramic capacitors, are selected as the output capacitors, a ripple injection method should be applied to provide the enough feedback voltage ripple. Refer to the [Ripple Injection](#) subsection for details.

The voltage rating of the capacitor should be twice the output voltage for a tantalum and 20% greater for aluminum electrolytic or OS-CON. The output capacitor RMS current is calculated in [Equation 5-11](#).

EQUATION 5-11:

$$I_{COUT(RMS)} = \frac{\Delta I_{L(PP)}}{\sqrt{12}}$$

The power dissipated in the output capacitor is:

EQUATION 5-12:

$$P_{DISS(COUT)} = I_{COUT(RMS)}^2 \times ESR_{COUT}$$

5.5 Input Capacitor Selection

The input capacitor for the power stage input V_{IN} should be selected for ripple current rating and voltage rating. Tantalum input capacitors may fail when subjected to high inrush currents, caused by turning the input supply on. A tantalum input capacitor's voltage rating should be at least two times the maximum input voltage to maximize reliability. Aluminum electrolytic, OS-CON, and multilayer polymer film capacitors can handle the higher inrush currents without voltage de-rating. The input voltage ripple will primarily depend on the input capacitor's ESR. The peak input current is equal to the peak inductor current, so:

EQUATION 5-13:

$$\Delta V_{IN} = I_{L(PK)} \times ESR_{CIN}$$

The input capacitor must be rated for the input current ripple. The RMS value of input capacitor current is determined at the maximum output current. Assuming the peak-to-peak inductor current ripple is low:

EQUATION 5-14:

$$I_{CIN(RMS)} \approx I_{OUT(MAX)} \times \sqrt{D \times (1 - D)}$$

The power dissipated in the input capacitor is:

EQUATION 5-15:

$$P_{DISS(CIN)} = I_{CIN(RMS)}^2 \times ESR_{CIN}$$

5.6 Ripple Injection

The V_{FB} ripple required for proper operation of the MIC28513's g_M amplifier and error comparator is 20 mV to 100 mV. However, the output voltage ripple is generally designed as 1% to 2% of the output voltage. If the feedback voltage ripple is so small that the g_M amplifier and error comparator can't sense it, then the MIC28513 will lose control and the output voltage is not regulated. In order to have some amount of V_{FB} ripple, a ripple injection method is applied for low output voltage ripple applications.

The applications are divided into three situations according to the amount of the feedback voltage ripple:

- Enough ripple at the feedback voltage due to the large ESR of the output capacitors ([Figure 5-4](#)). The converter is stable without any ripple injection.

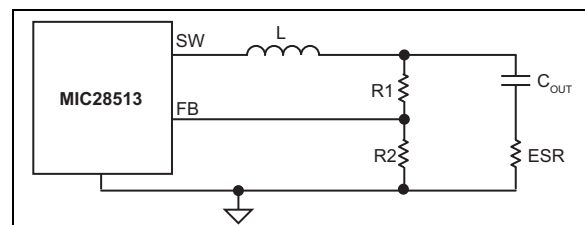


FIGURE 5-4: Enough Ripple at FB.

The feedback voltage ripple is:

MIC28513

EQUATION 5-16:

$$\Delta V_{FB(PP)} = \frac{R2}{R1 + R2} \times ESR_{C_{OUT}} \times \Delta I_{L(PP)}$$

Where:

$\Delta I_{L(PP)}$ Peak-to-Peak Value of the Inductor Current Ripple

- Inadequate ripple at the feedback voltage due to the small ESR of the output capacitors.

The output voltage ripple is fed into the FB pin through a feed-forward capacitor, C_{FF} in this situation, as shown in [Figure 5-5](#). The typical C_{FF} value is selected by using [Equation 5-17](#).

EQUATION 5-17:

$$R1 \times C_{FF} \approx \frac{10}{f_{SW}}$$

With the feed-forward capacitor, the feedback voltage ripple is very close to the output voltage ripple.

EQUATION 5-18:

$$\Delta V_{FB(PP)} \approx ESR \times \Delta I_{L(PP)}$$

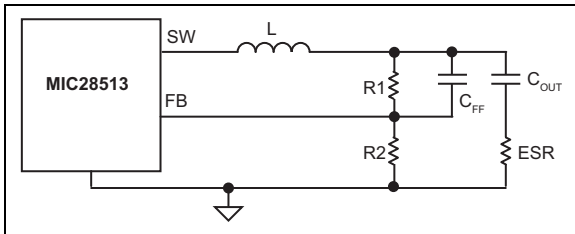


FIGURE 5-5: Inadequate Ripple at FB.

- Virtually no ripple at the FB pin voltage due to the very low ESR of the output capacitors.

In this situation, the output voltage ripple is less than 20 mV. Therefore, additional ripple is injected into the FB pin from the switching node SW via a resistor R_{INJ} and a capacitor C_{INJ} , as shown in [Figure 5-6](#).

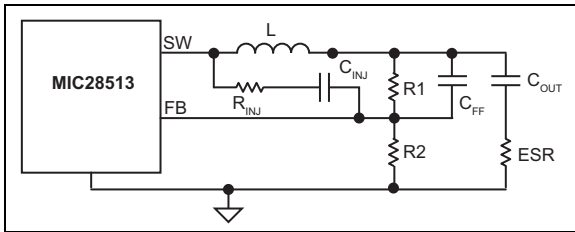


FIGURE 5-6: Invisible Ripple at FB.

The injected ripple is calculated via:

EQUATION 5-19:

$$\Delta V_{FB(PP)} = V_{IN} \times K_{div} \times D \times (1 - D) \times \frac{1}{f_{SW} \times \tau}$$

Where:

V_{IN} Power stage input voltage

D Duty cycle

f_{SW} Switching frequency

τ $(R1//R2//R_{INJ}) \times C_{FF}$

EQUATION 5-20:

$$K_{div} = \frac{R1//R2}{R_{INJ} + R1//R2}$$

In [Equation 5-19](#) and [Equation 5-20](#), it is assumed that the time constant associated with C_{FF} must be much greater than the switching period:

EQUATION 5-21:

$$\frac{1}{f_{SW} \times \tau} = \frac{T}{\tau} \ll 1$$

If the voltage divider resistors R1 and R2 are in the k Ω range, a C_{FF} of 1 nF to 100 nF can easily satisfy the large time constant requirements. Also, a 100 nF injection capacitor C_{INJ} is used in order to be considered as short for a wide range of the frequencies.

The process of sizing the ripple injection resistor and capacitors is as follows.

- Select C_{FF} to feed all output ripples into the feedback pin and make sure the large time constant assumption is satisfied. Typical choice of C_{FF} is 1 nF to 100 nF if R1 and R2 are in the k Ω range.
- Select R_{INJ} according to the expected feedback voltage ripple using [Equation 5-22](#):

EQUATION 5-22:

$$K_{div} = \frac{\Delta V_{FB(PP)}}{V_{IN}} \times \frac{f_{SW} \times \tau}{D \times (1 - D)}$$

The value of R_{INJ} is calculated using [Equation 5-23](#).

EQUATION 5-23:

$$R_{INJ} = (R1//R2) \times \left(\frac{1}{K_{div}} - 1 \right)$$

- Select C_{INJ} as 100 nF, which could be considered as short for a wide range of the frequencies.

5.7 Output Current Thermal Derating with SOA at High Input Voltage

For the MIC28513, at $V_{IN} = 45V$, $V_{OUT} = 5V$, $T_A = 25^\circ C$, the maximum output current $I_{OUT(MAX)}$ is about 3.3A because the $I_{OUT(MAX)}$ starts derating to less than 4A at a T_A around $0^\circ C$. The $I_{OUT(MAX)}$ further reduces as the ambient temperature increases. When output current derating starts, the $I_{OUT(MAX)}$ is inversely proportional to the device package thermal resistance θ_{JA} , and output voltage V_{OUT} , and is directly proportional to the factor $\eta/(1 - \eta)$ where η is the converter efficiency. The derate-starting ambient temperature depends on the

MIC28513 device maximum operating junction temperature $T_{J(MAX)}$, the maximum output current $I_{OUT(MAX)}$ without derating (which is the desired maximum output current limit I_{CLIM}), the output voltage V_{OUT} , the device package thermal resistance θ_{JA} , and the factor $(1 - \eta)/\eta$. For the examples of typical output current derating curves (SOA curves) for MIC28513, please refer to [Figure 2-21](#) and [Figure 2-22](#).

The maximum output current of MIC28513 with the device at the maximum junction temperature $T_{J(MAX)}$ operating over the ambient temperature T_A range can be estimated by [Equation 5-24](#).

EQUATION 5-24:

$$I_{OMAX(TJMAX)} = \left(-\frac{1}{\theta_{JA}} \times T_A + \left(\frac{T_{J(MAX)}}{\theta_{JA}} + P_{D(L)} \right) \right) \times \frac{\eta}{V_{OUT} \times (1 - \eta)}$$

Where:

θ_{JA} = Device Package Thermal Resistance, which is $30^\circ C/W$ for the 3 mm x 4 mm FCQFN-24LD.

η = Buck Converter Efficiency, for $V_{OUT} = 5V$ about 80% at $V_{IN} = 45V$, 85% at $V_{IN} = 36V$, 87% at $V_{IN} = 24V$.

$T_{J(MAX)}$ = Device Maximum Operating Junction Temperature, which is $125^\circ C$.

T_A = Ambient Temperature.

V_{OUT} = Output Voltage.

$P_{D(L)}$ = Inductor Power Dissipation due to DCR.

The inductor power dissipation due to DCR in [Equation 5-24](#) can be approximated by [Equation 5-25](#).

Because the maximum output current without thermal derating in the SOA curve is equal to the desired output current limit I_{CLIM} , the maximum output current in the SOA curve can be defined by [Equation 5-26](#).

EQUATION 5-25:

$$P_{D(L)} \approx I_{OUT}^2 \times DCR$$

Where:

I_{OUT} = Output Current.

DCR = Power Inductor DC Resistance.

EQUATION 5-26:

$$I_{OUT(MAX)} = \begin{cases} I_{CLIM} & \text{for } T_A \leq T_{A(DS)} \\ I_{OMAX(TJMAX)} & \text{for } T_A \geq T_{A(DS)} \end{cases}$$

Where:

I_{CLIM} = Desired Output Current Limit.

$T_{A(DS)}$ = Derate-Starting Ambient Temperature.

The derate-starting ambient temperature can be predicted using [Equation 5-27](#).

EQUATION 5-27:

$$T_{A(DS)} \approx T_{J(MAX)} - \left(I_{CLIM} \times V_{OUT} \times \frac{1 - \eta}{\eta} - P_{D(L)} \right) \times \theta_{JA}$$

MIC28513

If the $I_{OUT(MAX)}$ starts derating at an ambient temperature less than the user's actual maximum operating ambient temperature $T_{A(MAX,OP)}$, the $I_{OUT(MAX)}$ at $T_{A(MAX,OP)}$ in the SOA curve will be less than the desired output current limit I_{CLIM} . Then, the desired output current limit I_{CLIM} needs to be reduced to avoid the actual operating output current being out of the SOA curve boundary and to ensure safe operation. The output current limit in such condition can be estimated by [Equation 5-28](#).

EQUATION 5-28:

$$I_{CLIM} \leq \left[\frac{T_{J(MAX)} - T_{A(MAX,OP)}}{\theta_{JA}} + P_{D(L)} \right] \times \left[\frac{\eta}{V_{OUT} \times (1 - \eta)} \right]$$

Where:

$T_{A(MAX,OP)}$ = User's Actual Maximum Operating Ambient Temperature.

$T_{J(MAX)}$ = Device Maximum Operating Junction Temperature, which is 125°C.

θ_{JA} = Device Package Thermal Resistance, which is 30°C/W for the 3 mm x 4 mm FCQFN-24LD.

6.0 PCB LAYOUT GUIDELINES

PCB Layout is critical to achieve reliable, stable and efficient performance. A ground plane is required to control EMI and minimize the inductance in power and signal return paths.

Figure 6-1 is optimized from a small form-factor point of view and shows the top and bottom layers of a four-layer PCB. It is recommended to use Mid-Layer 1 as a continuous ground plane.

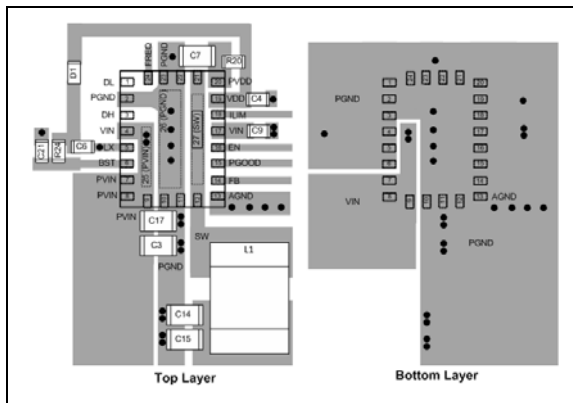


FIGURE 6-1: Top and Bottom Layers of a Four-Layer Board.

The following guidelines should be followed to ensure proper operation of the MIC28513 converter.

6.1 IC

- The analog ground pin (AGND) must be connected directly to the ground planes. Do not route the AGND pin to the PGND pin on the top layer.
- Place the IC close to the point-of-load (POL).
- Use copper planes to route the input and output power lines.
- Analog and power grounds should be kept separate and connected at only one location.

6.2 Input Capacitor

- Place the input capacitors on the same side of the board and as close to the PV_{IN} and PGND pins as possible.
- Place several vias to the ground plane close to the input capacitor ground terminal.
- Use either X7R or X5R dielectric input capacitors. Do not use Y5V or Z5U type capacitors.
- Do not replace the ceramic input capacitor with any other type of capacitor. Any type of capacitor can be placed in parallel with the input capacitor.
- If a Tantalum input capacitor is placed in parallel with the input capacitor, it must be recommended for switching regulator applications and the

operating voltage must be derated by 50%.

- In “Hot-Plug” applications, a Tantalum or Electrolytic bypass capacitor must be used to limit the overvoltage spike seen on the input supply with power is suddenly applied.

6.3 SW Node

- Do not route any digital lines underneath or close to the SW node.
- Keep the switch node (SW) away from the feedback (FB) pin.

6.4 Output Capacitor

- Use a copper island to connect the output capacitor ground terminal to the input capacitor ground terminal.
- Phase margin will change as the output capacitor value and ESR changes. Contact the factory if the output capacitor is different from what is shown in the BOM.
- The feedback trace should be separate from the power trace and connected as close as possible to the output capacitor. Sensing a long high-current load trace can degrade the DC load regulation.

6.5 Thermal Measurements

Measuring the IC’s case temperature is recommended to ensure it is within its operating limits. Although this might seem like a very elementary task, it is easy to get erroneous results. The most common mistake is to use the standard thermal couple that comes with a thermal meter. This thermal couple wire gauge is large, typically 22 gauge, and behaves like a heat sink, resulting in a lower case measurement.

Two methods of temperature measurement are using a smaller thermal couple wire or an infrared thermometer. If a thermal couple wire is used, it must be constructed of 36 gauge wire or higher (smaller wire size) to minimize the wire heat-sinking effect. In addition, the thermal couple tip must be covered in either thermal grease or thermal glue to make sure that the thermal couple junction is making good contact with the case of the IC. Omega brand thermal couple (5SC-TT-K-36-36) is adequate for most applications.

Wherever possible, an infrared thermometer is recommended. The measurement spot size of most infrared thermometers is too large for an accurate reading on a small form factor ICs. However, an IR thermometer from Optris has a 1 mm spot size, which makes it a good choice for measuring the hottest point on the case. An optional stand makes it easy to hold the beam on the IC for long periods of time.

For more information about the Evaluation board layout, please contact Microchip sales.

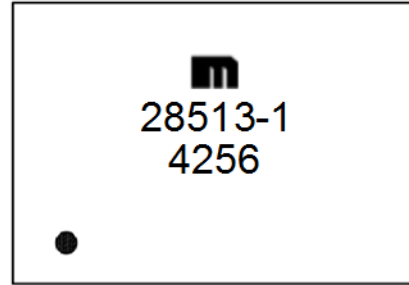
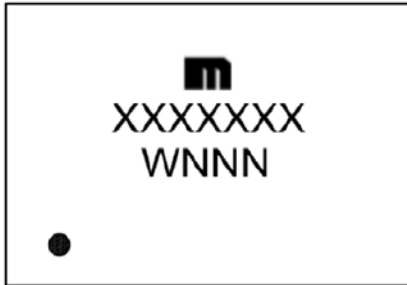
MIC28513

7.0 PACKAGING INFORMATION

7.1 Package Marking Information

24-Lead FQFN*

Example



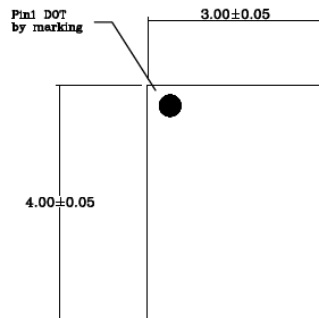
Legend:	XX...X	Product code or customer-specific information
	Y	Year code (last digit of calendar year)
	YY	Year code (last 2 digits of calendar year)
	WW	Week code (week of January 1 is week '01')
	NNN	Alphanumeric traceability code
	(e3)	Pb-free JEDEC® designator for Matte Tin (Sn)
	*	This package is Pb-free. The Pb-free JEDEC designator (e3) can be found on the outer packaging for this package.
	•, ▲, ▼	Pin one index is identified by a dot, delta up, or delta down (triangle mark).
Note:	In the event the full Microchip part number cannot be marked on one line, it will be carried over to the next line, thus limiting the number of available characters for customer-specific information. Package may or may not include the corporate logo.	
	Underbar (¯) and/or Overbar (¯) symbol may not be to scale.	

24-Lead FQFN 3 mm x 4 mm Package Outline and Recommended Land Pattern

TITLE

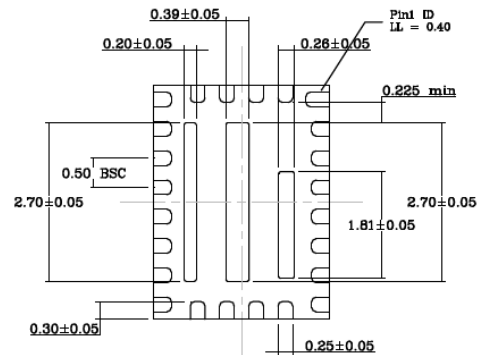
24 LEAD FQFN 3x4mm PACKAGE OUTLINE & RECOMMENDED LAND PATTERN

DRAWING #	FQFN34-24LD-PL-2	UNIT	MM
Lead Frame	Copper	Lead Finish	Matte Tin



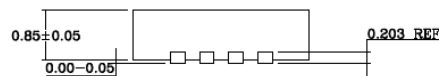
Top View

Note 1,2,3



Bottom View

Note 1,2,3



Side View

Note 1,2,3

NOTE:

1. MAX PACKAGE WARPAGE IS 0.05mm.
2. MAX ALLOWABLE BURR IS 0.076mm IN ALL DIRECTIONS.
3. PIN #1 IS ON TOP WILL BE LASER MARKED.
4. RED CIRCLES IN LAND PATTERN REPRESENT THERMAL VIAs & SHOULD BE CONNECTED TO GND FOR MAXIMUM PERFORMANCE. SIZE IS 0.30-0.35mm WITH 0.80mm PITCH.
5. SHADED AREA RECTANGLES REPRESENT SOLDER STENCIL OPENING ON EXPOSED METAL TRACE.
6. MAGENTA & BLUE COLORED RECTANGLES REPRESENT DIFFERENT POTENTIAL, DO NOT CONNECT TO GND.
7. BLACK COLORED RECTANGLES REPRESENT DIFFERENT IOs. DO NOT CONNECT TOGETHER.
8. RECOMMENDED LAND PATTERN TOLERANCE IS 0.02mm UNLESS SPECIFIED.
9. SEE RECOMMENDED LAND PATTERN ON PAGE 2.

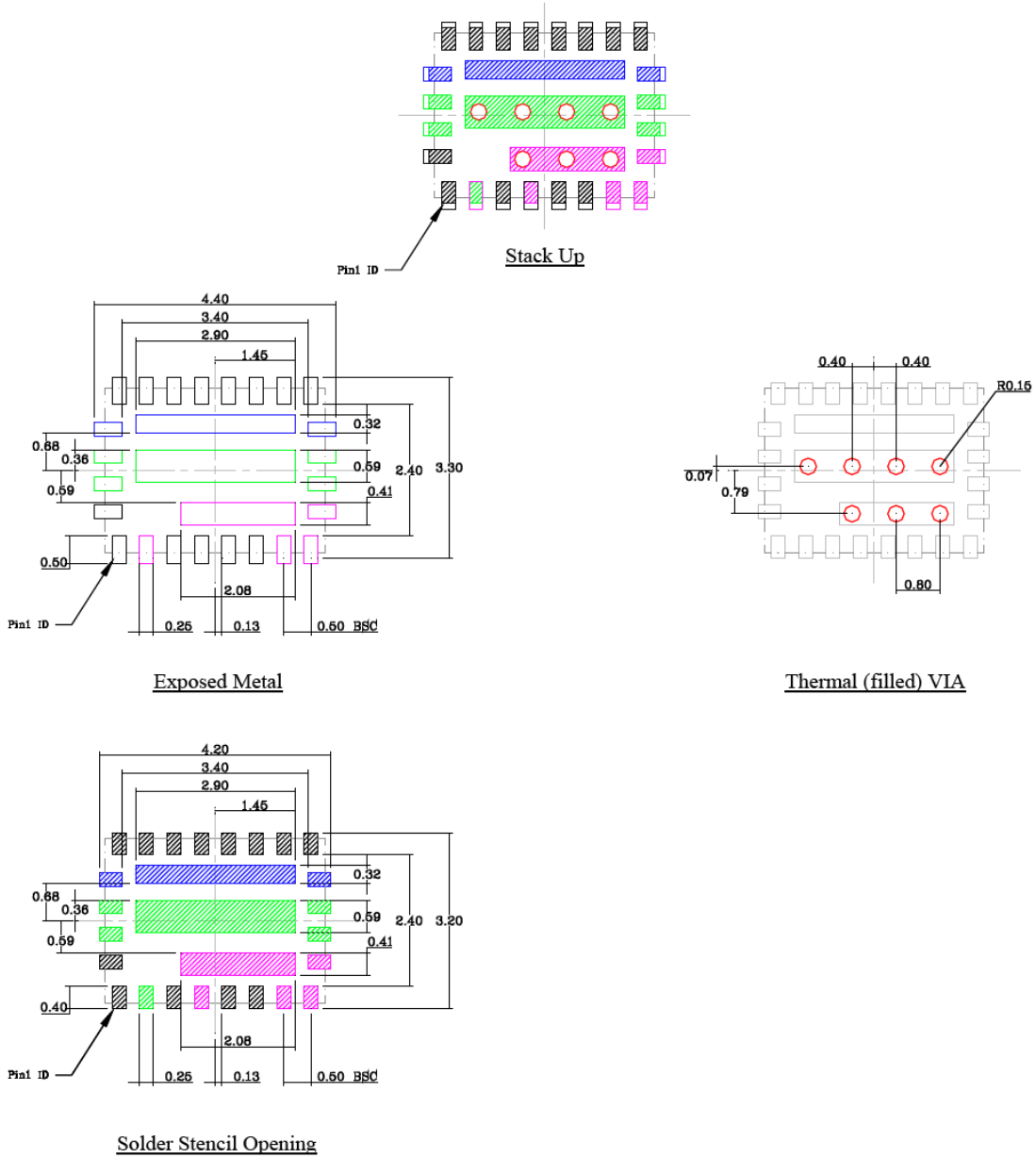
Note: For the most current package drawings, please see the Microchip Packaging Specification located at <http://www.microchip.com/packaging>.

MIC28513

POD-Land Pattern Doc #: FQFN34-24LD-PL-2-E

Recommended Land Pattern

Note: 4.5,6,7



Note: For the most current package drawings, please see the Microchip Packaging Specification located at <http://www.microchip.com/packaging>.

APPENDIX A: REVISION HISTORY

Revision A (May 2016)

- Converted Micrel document MIC28513 to Microchip data sheet template DS20005522A.
- Minor text changes throughout.

Revision B (July 2018)

- Updated V_{IN} value in [Typical Application Circuit](#).
- Updated [Equation 4-3](#), [Equation 5-6](#), [Equation 5-10](#).
- Updated [Absolute Maximum Ratings](#) †.
- Updated content in [Section 4.5, Current Limit](#).
- Added [Section 4.6, Output Current Thermal Derating](#).
- Added [Section 5.7, Output Current Thermal Derating with SOA at High Input Voltage](#).
- Added [Section 7.1, Package Marking Information](#).
- Various typographical edits.

MIC28513

NOTES:

PRODUCT IDENTIFICATION SYSTEM

To order or obtain information, e.g., on pricing or delivery, contact your local Microchip representative or sales office.

<u>PART NO.</u>	-X	X	XX	-XX
Device	Architecture	Temperature	Package	Media Type
Device:	MIC28513:	45V _{IN} , 4A Synchronous Buck Regulator		
Architecture:	1 =	HyperLight Load		
	2 =	Hyper Speed Control		
Temperature:	Y =	-40°C to +125°C		
Package:	FL =	24-Pin 3 mm x 4 mm QFN; Note 1		
Media Type:	T5 =	500/Reel		
	TR =	5,000/Reel		
Note 1: QFN is a lead-free package. Pb-Free lead finish is Matte Tin.				
Examples:				
a) MIC28513-1YFL-T5: 45V _{IN} , 2A Synchronous Buck Regulator, HyperLight Load, -40°C to +125°C Junction Temperature Range, 24LD QFN, 500/Reel				
b) MIC28513-1YFL-TR: 45V _{IN} , 2A Synchronous Buck Regulator, HyperLight Load, -40°C to +125°C Junction Temperature Range, 24LD QFN, 5,000/Reel				
c) MIC28513-2YFL-T5: 45V _{IN} , 2A Synchronous Buck Regulator, Hyper Speed Control, -40°C to +125°C Junction Temperature Range, 24LD QFN, 500/Reel				
d) MIC28513-2YFL-TR: 45V _{IN} , 2A Synchronous Buck Regulator, Hyper Speed Control, -40°C to +125°C Junction Temperature Range, 24LD QFN, 5,000/Reel				
Note 1: Tape and Reel identifier only appears in the catalog part number description. This identifier is used for ordering purposes and is not printed on the device package. Check with your Microchip Sales Office for package availability with the Tape and Reel option.				

MIC28513

NOTES:

Note the following details of the code protection feature on Microchip devices:

- Microchip products meet the specification contained in their particular Microchip Data Sheet.
- Microchip believes that its family of products is one of the most secure families of its kind on the market today, when used in the intended manner and under normal conditions.
- There are dishonest and possibly illegal methods used to breach the code protection feature. All of these methods, to our knowledge, require using the Microchip products in a manner outside the operating specifications contained in Microchip's Data Sheets. Most likely, the person doing so is engaged in theft of intellectual property.
- Microchip is willing to work with the customer who is concerned about the integrity of their code.
- Neither Microchip nor any other semiconductor manufacturer can guarantee the security of their code. Code protection does not mean that we are guaranteeing the product as “unbreakable.”

Code protection is constantly evolving. We at Microchip are committed to continuously improving the code protection features of our products. Attempts to break Microchip's code protection feature may be a violation of the Digital Millennium Copyright Act. If such acts allow unauthorized access to your software or other copyrighted work, you may have a right to sue for relief under that Act.

Information contained in this publication regarding device applications and the like is provided only for your convenience and may be superseded by updates. It is your responsibility to ensure that your application meets with your specifications. MICROCHIP MAKES NO REPRESENTATIONS OR WARRANTIES OF ANY KIND WHETHER EXPRESS OR IMPLIED, WRITTEN OR ORAL, STATUTORY OR OTHERWISE, RELATED TO THE INFORMATION, INCLUDING BUT NOT LIMITED TO ITS CONDITION, QUALITY, PERFORMANCE, MERCHANTABILITY OR FITNESS FOR PURPOSE. Microchip disclaims all liability arising from this information and its use. Use of Microchip devices in life support and/or safety applications is entirely at the buyer's risk, and the buyer agrees to defend, indemnify and hold harmless Microchip from any and all damages, claims, suits, or expenses resulting from such use. No licenses are conveyed, implicitly or otherwise, under any Microchip intellectual property rights unless otherwise stated.

Microchip received ISO/TS-16949:2009 certification for its worldwide headquarters, design and wafer fabrication facilities in Chandler and Tempe, Arizona; Gresham, Oregon and design centers in California and India. The Company's quality system processes and procedures are for its PIC® MCUs and dsPIC® DSCs, KEELoc® code hopping devices, Serial EEPROMs, microperipherals, nonvolatile memory and analog products. In addition, Microchip's quality system for the design and manufacture of development systems is ISO 9001:2000 certified.

**QUALITY MANAGEMENT SYSTEM
CERTIFIED BY DNV
= ISO/TS 16949 =**

Trademarks

The Microchip name and logo, the Microchip logo, AnyRate, AVR, AVR logo, AVR Freaks, BitCloud, chipKIT, chipKIT logo, CryptoMemory, CryptoRF, dsPIC, FlashFlex, flexPWR, Helder, JukeBlox, KeeLoq, Klear, LANCheck, LINK MD, maXStylus, maXTouch, MediaLB, megaAVR, MOST, MOST logo, MPLAB, OptoLyzer, PIC, picoPower, PICSTART, PIC32 logo, Prochip Designer, QTouch, SAM-BA, SpyNIC, SST, SST Logo, SuperFlash, tinyAVR, UNI/O, and XMEGA are registered trademarks of Microchip Technology Incorporated in the U.S.A. and other countries.

ClockWorks, The Embedded Control Solutions Company, EtherSynch, Hyper Speed Control, HyperLight Load, IntellIMOS, mTouch, Precision Edge, and Quiet-Wire are registered trademarks of Microchip Technology Incorporated in the U.S.A.

Adjacent Key Suppression, AKS, Analog-for-the-Digital Age, Any Capacitor, AnyIn, AnyOut, BodyCom, CodeGuard, CryptoAuthentication, CryptoAutomotive, CryptoCompanion, CryptoController, dsPICDEM, dsPICDEM.net, Dynamic Average Matching, DAM, ECAN, EtherGREEN, In-Circuit Serial Programming, ICSP, INICnet, Inter-Chip Connectivity, JitterBlocker, KlearNet, KlearNet logo, memBrain, Mindi, MiWi, motorBench, MPASM, MPF, MPLAB Certified logo, MPLIB, MPLINK, MultiTRAK, NetDetach, Omniscient Code Generation, PICDEM, PICDEM.net, PICKit, PICtail, PowerSmart, PureSilicon, QMatrix, REAL ICE, Ripple Blocker, SAM-ICE, Serial Quad I/O, SMART-I.S., SQI, SuperSwitcher, SuperSwitcher II, Total Endurance, TSHARC, USBCheck, VariSense, ViewSpan, WiperLock, Wireless DNA, and ZENA are trademarks of Microchip Technology Incorporated in the U.S.A. and other countries.

SQTP is a service mark of Microchip Technology Incorporated in the U.S.A.

Silicon Storage Technology is a registered trademark of Microchip Technology Inc. in other countries.

GestIC is a registered trademark of Microchip Technology Germany II GmbH & Co. KG, a subsidiary of Microchip Technology Inc., in other countries.

All other trademarks mentioned herein are property of their respective companies.

© 2016-2018, Microchip Technology Incorporated, All Rights Reserved.

ISBN: 978-1-5224-3361-3



MICROCHIP

Worldwide Sales and Service

AMERICAS

Corporate Office
2355 West Chandler Blvd.
Chandler, AZ 85224-6199
Tel: 480-792-7200
Fax: 480-792-7277
Technical Support:
<http://www.microchip.com/support>
Web Address:
www.microchip.com

Atlanta
Duluth, GA
Tel: 678-957-9614
Fax: 678-957-1455

Austin, TX
Tel: 512-257-3370

Boston
Westborough, MA
Tel: 774-760-0087
Fax: 774-760-0088

Chicago
Itasca, IL
Tel: 630-285-0071
Fax: 630-285-0075

Dallas
Addison, TX
Tel: 972-818-7423
Fax: 972-818-2924

Detroit
Novi, MI
Tel: 248-848-4000

Houston, TX
Tel: 281-894-5983

Indianapolis
Noblesville, IN
Tel: 317-773-8323
Fax: 317-773-5453
Tel: 317-536-2380

Los Angeles
Mission Viejo, CA
Tel: 949-462-9523
Fax: 949-462-9608
Tel: 951-273-7800

Raleigh, NC
Tel: 919-844-7510

New York, NY
Tel: 631-435-6000

San Jose, CA
Tel: 408-735-9110
Tel: 408-436-4270

Canada - Toronto
Tel: 905-695-1980
Fax: 905-695-2078

ASIA/PACIFIC

Australia - Sydney
Tel: 61-2-9868-6733

China - Beijing
Tel: 86-10-8569-7000

China - Chengdu
Tel: 86-28-8665-5511

China - Chongqing
Tel: 86-23-8980-9588

China - Dongguan
Tel: 86-769-8702-9880

China - Guangzhou
Tel: 86-20-8755-8029

China - Hangzhou
Tel: 86-571-8792-8115

China - Hong Kong SAR
Tel: 852-2943-5100

China - Nanjing
Tel: 86-25-8473-2460

China - Qingdao
Tel: 86-532-8502-7355

China - Shanghai
Tel: 86-21-3326-8000

China - Shenyang
Tel: 86-24-2334-2829

China - Shenzhen
Tel: 86-755-8864-2200

China - Suzhou
Tel: 86-186-6233-1526

China - Wuhan
Tel: 86-27-5980-5300

China - Xian
Tel: 86-29-8833-7252

China - Xiamen
Tel: 86-592-2388138

China - Zhuhai
Tel: 86-756-3210040

ASIA/PACIFIC

India - Bangalore
Tel: 91-80-3090-4444

India - New Delhi
Tel: 91-11-4160-8631

India - Pune
Tel: 91-20-4121-0141

Japan - Osaka
Tel: 81-6-6152-7160

Japan - Tokyo
Tel: 81-3-6880-3770

Korea - Daegu
Tel: 82-53-744-4301

Korea - Seoul
Tel: 82-2-554-7200

Malaysia - Kuala Lumpur
Tel: 60-3-7651-7906

Malaysia - Penang
Tel: 60-4-227-8870

Philippines - Manila
Tel: 63-2-634-9065

Singapore
Tel: 65-6334-8870

Taiwan - Hsin Chu
Tel: 886-3-577-8366

Taiwan - Kaohsiung
Tel: 886-7-213-7830

Taiwan - Taipei
Tel: 886-2-2508-8600

Thailand - Bangkok
Tel: 66-2-694-1351

Vietnam - Ho Chi Minh
Tel: 84-28-5448-2100

EUROPE

Austria - Wels
Tel: 43-7242-2244-39
Fax: 43-7242-2244-393

Denmark - Copenhagen
Tel: 45-4450-2828
Fax: 45-4485-2829

Finland - Espoo
Tel: 358-9-4520-820

France - Paris
Tel: 33-1-69-53-63-20
Fax: 33-1-69-30-90-79

Germany - Garching
Tel: 49-8931-9700

Germany - Haan
Tel: 49-2129-3766400

Germany - Heilbronn
Tel: 49-7131-67-3636

Germany - Karlsruhe
Tel: 49-721-625370

Germany - Munich
Tel: 49-89-627-144-0
Fax: 49-89-627-144-44

Germany - Rosenheim
Tel: 49-8031-354-560

Israel - Ra'anana
Tel: 972-9-744-7705

Italy - Milan
Tel: 39-0331-742611
Fax: 39-0331-466781

Italy - Padova
Tel: 39-049-7625286

Netherlands - Drunen
Tel: 31-416-690399
Fax: 31-416-690340

Norway - Trondheim
Tel: 47-7289-7561

Poland - Warsaw
Tel: 48-22-3325737

Romania - Bucharest
Tel: 40-21-407-87-50

Spain - Madrid
Tel: 34-91-708-08-90
Fax: 34-91-708-08-91

Sweden - Gothenberg
Tel: 46-31-704-60-40

Sweden - Stockholm
Tel: 46-8-5090-4654

UK - Wokingham
Tel: 44-118-921-5800
Fax: 44-118-921-5820